

Journal Pre-proof

Chlorination and bromination of 1,3-diphenylguanidine and 1,3-*di-o*-tolylguanidine: Kinetics, transformation products and toxicity assessment

Benigno J. Sieira, Rosa Montes, Arnaud Touffet, Rosario Rodil, Rafael Cela, Hervé Gallard, José Benito Quintana



PII: S0304-3894(19)31544-4

DOI: <https://doi.org/10.1016/j.jhazmat.2019.121590>

Reference: HAZMAT 121590

To appear in: *Journal of Hazardous Materials*

Received Date: 30 July 2019

Revised Date: 17 October 2019

Accepted Date: 31 October 2019

Please cite this article as: { doi: <https://doi.org/>

This is a PDF file of an article that has undergone enhancements after acceptance, such as the addition of a cover page and metadata, and formatting for readability, but it is not yet the definitive version of record. This version will undergo additional copyediting, typesetting and review before it is published in its final form, but we are providing this version to give early visibility of the article. Please note that, during the production process, errors may be discovered which could affect the content, and all legal disclaimers that apply to the journal pertain.

© 2019 Published by Elsevier.

CHLORINATION AND BROMINATION OF 1,3-DIPHENYLGUANIDINE AND 1,3-DI-O-TOLYLGUANIDINE: KINETICS, TRANSFORMATION PRODUCTS AND TOXICITY ASSESSMENT

Benigno J. Sieira ¹, Rosa Montes ¹, Arnaud Touffet ², Rosario Rodil ¹, Rafael Cela ¹, Hervé Gallard ^{2*}, José Benito Quintana ^{1*}

¹ Department of Analytical Chemistry, Nutrition and Food Sciences, Institute of Food Analysis and Research (IIAA), Universidade de Santiago de Compostela, R/ Constantino Candeira S/N, 15782 – Santiago de Compostela (Spain)

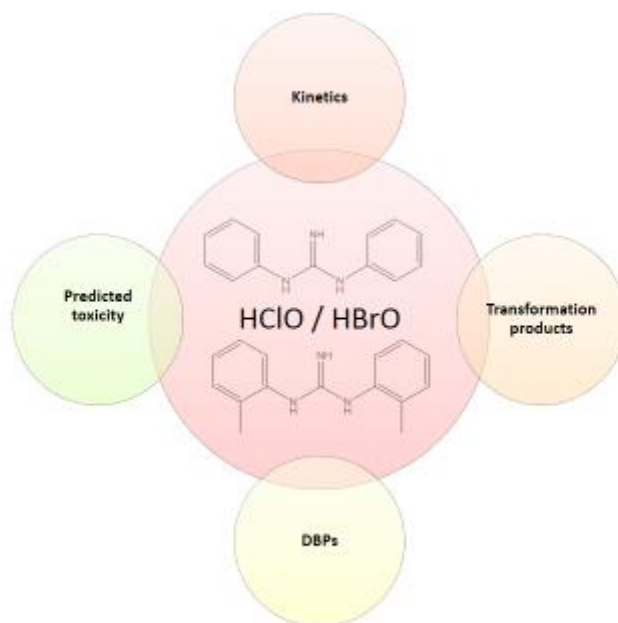
² Institute de Chimie des Milieux et des Matériaux de Poitiers (IC2MP), École Nationale Supérieure d'Ingénieurs de Poitiers (ENSIP), Université de Poitiers, 1, rue Marcel Doré, TSA 41105, 86073 – Poitiers (France)

* Corresponding authors:

Hervé Gallard: herve.gallard@univ-poitiers.fr

José Benito Quintana. jb.quintana@usc.es

Graphical abstract



Highlights

- DPG and DTG react rapidly with chlorine and bromine
- The pH dependence of the reaction was modelled
- Several transformation products were identified by LC-QTOF
- Chloroform and dichloroacetonitrile are also produced
- TPs are more toxic than DPG and DTG

Abstract

This work investigates the chlorination and bromination of two rubber and polymer related chemicals, which have emerged as relevant water contaminants, i.e. 1,3-di-*o*-tolylguanidine (DTG) and 1,3-diphenylguanidine (DPG). Kinetic constants at different pH values were obtained and modelled, taking into account the pK_a values of DTG/DPG and HClO, showing that the maximum reaction rate ($k_{app} > 10^4 \text{ M}^{-1} \text{ s}^{-1}$) is obtained at pH values 8.8 for DPG and 9.1 for DTG. Bromination is also very fast, although unlike chlorination, deviation from the model was observed at neutral pH, which was

attributed to formation of metastable transformation product (TP). A total of 35 TPs, corresponding to halogenation, hydroxylation, formation of monophenylguanidine derivatives and cyclization reactions, were tentatively identified. Furthermore it was found that chloroform can be formed up to a 25% molar yield, while dichloroacetonitrile was formed into less than a 3% yield. Several ecotoxicological endpoints were predicted by quantitative structure–activity relationship models (QSAR) for the TPs, some of which were predicted to be more toxic than DPG/DTG. Also a chlorinated solution investigated by a *Vibrio Fisheri* acute toxicity test, confirmed that toxicity increases with chlorination.

Keywords

Halogenation; transformation products; high-resolution mass spectrometry (HRMS); ecotoxicity; disinfection by-products.

1. Introduction

Polar organic compounds, if persistent, spread along the water cycle, even becoming a human health problem if that substances reach drinking waters (Hernández et al. 2015, Reemtsma et al. 2016, Schulze et al. 2019). 1,3-Di-*o*-tolylguanidine (DTG) and 1,3-diphenylguanidine (DPG) are chemicals used as accelerators in the vulcanization processes of rubber and other polymers manufacture, with a registered production in Europe, according to the REACH dossiers, in the 100-1000 tons (DTG) and 1000-10,000 tons (DPG) (ECHA 2018a, b). However, so far, little information about their

environmental (particularly water) occurrence is available. A first study from Montes et al. (Montes et al. 2017), in the frame of the project PROMOTE (Metcalf et al. 2003), reported DTG occurring in environmental water samples across Europe by liquid chromatography-high resolution mass spectrometry (LC-HRMS) screening. Later on, within the same project, it has been shown that DPG as well as DTG occur in different water compartments at the ng L^{-1} level (Montes et al. 2019, Schulze et al. 2019). Zahn et al. have recently shown that, when considering natural processes, DPG (DTG was not considered in that study) photolyzes and reacts with manganese oxide, but does not biodegrade and is stable to hydrolysis (Zahn et al. 2019). Furthermore, this compound has been identified in drinking water in China at 0.7 mg L^{-1} , migrating from polyethylene pipes (Tang et al. 2015) and, more recently, has also been recently identified as being the major chemical leaching from tire wear particles (Hübner et al. 2019, Zahn et al. 2019). Furthermore, there is some literature that describes DTG and DPG toxicity and pharmacological activity in mice and rats (Jaramillo-Ioranca and Esram 2015, Lamy et al. 2010).

Yet, the possible reaction of both chemicals with chemical oxidants used in drinking water treatment plants (DWTPs) and wastewater treatment plants (WWTPs) has not been studied so far. Several disinfection techniques and processes are employed in DWTPs and WWTPs. Among them, chlorine is the oxidant used in the vast majority of DWTPs in Europe, and also in some WWTPs to a minor extent (Benitez et al. 2011, Quintana et al. 2014). Although chlorine is effective to inactivate bacteria, the formation of possible harmful transformation products (TPs), including well-known disinfection byproducts (DBPs), as e.g. trihalomethanes, needs to be taken into account (Acero et al. 2013, Postigo and Richardson 2014, Quintana et al. 2014, Rodil et

al. 2012). Such TPs (including DBPs) may in some cases be more (eco)toxic than the precursor chemicals themselves (Postigo and Richardson 2014, Quintana et al. 2014). Therefore, their identification is necessary in order to obtain a relevant interpretation of the reaction.

Thus, the aim of this work was to perform a comprehensive study about the chlorination of DTG and DPG in water. This includes a kinetic study and modelling, identification of TPs (including those formed by bromination, since hypobromite is rapidly formed from bromide into solution during chlorination (Benitez et al. 2011)) by LC-HRMS, quantification of the yield of known DBPs formed and preliminary (eco)toxicological assessment.

2. Materials and methods

2.1. Chemicals and stock solutions

DTG (99%) and DPG (97%) were purchased from Sigma-Aldrich (Steinheim, Germany) and stock solutions were prepared in ultra-pure water. Ultra-pure water was obtained directly in the lab from a Milli-Q Gradient A-10 system (Millipore, Bedford, MA, USA). All solutions and dilutions necessary for the experiments were done in ultra-pure water until desired concentration.

Sodium hypochlorite (8-14% Cl₂), ammonium chloride (> 99%) and potassium phosphate dibasic trihydrate (> 99%) were obtained from Sigma-Aldrich. Sodium thiosulfate (99.5%) and potassium bromide were from ACS Acros Organics (Thermo Fisher Scientific, Waltham, MA, USA) and potassium di-hydrogen phosphate (99.5%) was from Panreac (Barcelona, Spain). Standard solutions of chloroform and haloacetonitriles (HANs) were prepared from EPA 551B Halogenated Volatiles Mix supplied from Supelco. The exact nominal free chlorine content employed was regularly determined spectrophotometrically by measuring the hypochlorite anion absorption at 292 nm ($\epsilon = 350 \text{ L}^{-1} \text{ cm}^{-1}$) (Johnson and Melbourne 1996) of the stock solution (pH >10).

2.2. Real samples

Two samples were used to study the extent of the chlorination reaction with a real matrix. A surface water sample was collected from the River Sarela in Santiago de Compostela (pH 6.8, Dissolved Organic Carbon: 2.42 mg L⁻¹, chloride: 7.98 mg L⁻¹, bromide: 0.043 mg L⁻¹). A wastewater effluent was collected from a WWTP comprising a primary and a secondary conventional sludge treatment (pH: 7.5, Dissolved Organic

Carbon: 14.1 mg L⁻¹, chloride: 23.1 mg L⁻¹, bromide: 0.075 mg L⁻¹). Dissolved organic carbon was measured with a Shimadzu 5000A TOC analyzer (Duisburg, Germany), while bromide and chloride were determined with a Metrohm 850 Professional Ion Chromatograph (Zofingen, Switzerland).

2.3. Chlorination experiments

Chlorination of DTG and DPG were performed individually in 100 mL amber closed vials at room temperature. Also, experiments without chlorine were prepared as a control.

Experiments to study chlorination kinetics were performed in a similar way, but with lower compound concentrations (1 μM), an excess of chlorine (10 μM, 20 μM or 50 μM) and different pH of sample (5-12) being considered in 10 mM phosphate buffer and NaOH for very basic pHs. Aliquots of 1 mL were taken at different reaction times and the reaction stopped with 20 μL of 0.01 M sodium thiosulfate before residual concentration of guanidine was analysed by liquid chromatography-photodiode array detection (LC-PDA). Ammonium chloride (1 mM) was used in some experiments as “soft” quenching method as being selective to free chlorine and as to avoid any Na₂S₂O₃-induced back reaction that could interfere with determination of rate constant (Dodd and Huang 2004). An experiment was also performed without stopping the reaction and aliquots were manually injected at different reaction times using a Rheodyne valve in the LC-PDA system.

Experiments were performed at room temperature (22 ±1°C). The pH was measured before and after the experiment, and variation was less than 0.1 unit. Free active chlorine was analysed by DPD colorimetric method (Clesceri et al. 1998) at the end of

reaction time. Chlorine consumption was usually below 10% and pseudo-first-order plots were always linear (see Figure S1 for examples).

Additional experiments for the identification of TPs (performed in triplicate) were carried out with a similar procedure. For these experiments, ultrapure water adjusted at pH 7.0 was used, spiked with the compound at 10 μM , and initial chlorine dose set to 100 μM . TPs were identified after reduction by ascorbic acid for reaction times of 30 s, 1 min, 2 min, 5 min, 10 min and 30 min.

DBPs formation potentials (chloroform and haloacetonitriles) were determined for a reaction time of 2 days at pH 7.0 in ultrapure water with an initial concentration (of either DPG or DTG) of 10 μM and molar chlorine to guanidine ratios of 1, 10 and 100 in headspace-free conditions.

2.4. Bromination experiments

Bromination experiments were performed under the same conditions as chlorination, in order to determine apparent rate constants and detect TPs that can be produced in bromide containing waters. Bromine was generated in the lab according to the procedure described by Benitez et al. (Benitez et al. 2011). Briefly, bromine was produced from the reaction between 9 mM HOCl and 10 mM potassium bromide. The yield of this reaction was followed spectrophotometrically (hypobromite anion maximum absorption wavelength at 329 nm with an $\epsilon = 332 \text{ M}^{-1} \text{ cm}^{-1}$ at pH above 11.5) (Benitez et al. 2011).

Kinetics of bromination were studied as for chlorination for pH values ranging from 5 to 9 using direct method in batch reactor with an excess of bromine (10 to 100 μM) compared to 1 μM DPG or DTG solution (see Figure S2 for examples of bromination of

DPG). Apparent rate constants were also determined by using the competition kinetics method (Acero et al., 2005) with 4-bromophenol (BP) in pH 8 - 11 range or 2,4,6-tribromophenol (TBP) at pH 7.0 and 8.0 as reference compounds (see Figure S3). In this method, different concentrations of bromine from 0 to 10 μM were introduced in 25 mL of a 10 mM phosphate buffer solution containing 5 μM DPG or DTG and 5 μM reference compound (either BP or TBP). Residual concentrations of organic compounds were determined by LC-PDA. Apparent rate constants of BP and TBP were calculated for each pH from intrinsic rate constants compiled by Heeb et al. (2014) and $\text{pK}_a_{\text{HOBr/BrO}^-} = 8.8$. Values are given in Table S3 and S4. An apparent rate constant of $2063 \text{ M}^{-1} \text{ s}^{-1}$ was determined for the reaction of bromine with TBP at pH 6.94 by direct method using 20 μM bromine and 1 μM TBP (Figure S4); value similar to $2100 \text{ M}^{-1} \text{ s}^{-1}$ determined by Acero et al. (2005) and used in this study.

2.5. Liquid chromatography - photodiode array detection (LC-PDA)

The chlorination kinetic study was followed by analysing the samples in a LC-PDA system. The instrument was a Waters 2695 LC (Milford, MA, USA) equipped with a degasser, binary high-pressure pump, LC column oven and an autosampler. The PDA was a Waters 2996 equipped with a deuterium lamp. DPG was monitored at 235 nm, whereas DTG, BP and TBP were measured at 225 nm.

The LC column used was a 250 mm x 4.6 mm; 5 μm Kinetex EVO C18 (Phenomenex, Torrance, CA, USA) at a flow rate of 1 mL min^{-1} . Mobile phase consisted in Milli-Q water (eluent A) and acetonitrile (eluent B), both acidified with 0.1 % formic acid. Gradient was as follows: 0 min, 5% B; 10 min, 100% B; 12 min, 100% B; 12.10 min, 5%

B; 20 min, 5% B. Injection volume was set to 50 μL . Instrument control and data treatment were done with Empower software (Waters).

2.6. LC-HRMS

The system used for the determination of TPs was an Agilent 1200 Series LC (Agilent Technologies, Santa Clara, CA, USA) equipped with a degasser, a binary high-pressure pump, LC column oven and an autosampler. This LC system was interfaced to an Agilent 6520 Series Quadrupole-Time of Flight (QTOF) MS equipped with a Dual Electrospray (Dual-ESI) ion source.

The LC column was a Luna 150 mm x 2 mm; 3 μm C18 (2) (Phenomenex) at a flow of mobile phase of 0.2 mL min^{-1} , and column temperature established at 35 $^{\circ}\text{C}$. Mobile phase and gradient used are the same as described in Section 2.5. Injection volume was set at 10 μL .

For the QTOF, Nitrogen (99.999%) used for nebulising and drying gas was supplied by a nitrogen generator (Erre Due Srl, Livorno, Italy). Collision-Induced Dissociation (CID) in tandem mass spectrometry analysis (MS/MS) was performed with Nitrogen (99.9995%) purchased from Praxair (Santiago de Compostela, Spain) as collision gas. ESI source operated in positive (no TPs were detected in negative) polarity and its parameters were as follows: gas temperature 350 $^{\circ}\text{C}$; drying gas 5 L min^{-1} ; nebulizer 42 psig, capillary 4000 V; fragmentor 120 V; skimmer 65 V; and octapole RF 750 V. Instrument acquired MS spectra in centroid mode and operated at 2 GHz (extended-dynamic range), which provided a Full Width at Half Maximum (FWHM) resolution of ca. 4500 at m/z 121 and ca. 11000 at m/z 922, scan range: 70-1000 m/z . The manufacturer reference solution was also infused during every run and ionized with

the second sprayer of the Dual-ESI at 5 psig, to calibrate automatically and keep the mass accuracy. In this solution, two masses, m/z 121.0509 and 922.0098 for ESI (+) were used for m/z -axis continuous recalibration.

Instrument control and data treatment were done with different software included in the MassHunter package (Agilent Technologies). Determination of TPs was performed as described elsewhere (Carpinteiro et al. 2017). Briefly, the algorithm “Find by Molecular Feature” from the MassHunter Qualitative (Agilent Technologies) software was used to generate a list of features (chromatographic peaks and m/z values) with a response higher than 1000 counts. Data obtained was then analysed with the software Mass Profiler Professional (Agilent Technologies) that compares the intensity of those features at different reaction times, where features whose intensity increases as compared to time 0 can be possible TPs. Then, formulas were generated for those features. The isotope pattern matching as well as error between the experimental m/z values and those calculated (from the generated formula) is grouped by the software to provide a score in percentage, in which 100% would indicate a perfect match.

Tandem mass spectrometry (MS/MS) analysis were obtained for the structure elucidation of the TPs structures, using CID with different collision energies between 10 and 40 V.

2.7. Determination of DBPs

Chloroform was analysed by headspace injection and gas chromatography coupled to mass spectrometry detection (GC-MS). Analysis was performed by using a CTC Analytics Combi Pal autosampler with an Agilent 7890 GC and an Agilent 5975C mass spectrometer. 10 mL of sample were poured in 20 mL headspace vials containing 10 μ L

of 1M ascorbic acid to quench residual chlorine. Vials were heated at 50°C and stirred at 500 rpm for 10 min before 2.5 mL gas phase was injected into the gas chromatography in pulsed split mode (ratio 1:10). The analytical column was an Agilent HP-5MS column (30 m x 0.25 mm; film thickness 1 µm). Retention time of chloroform was 3.8 min for temperature program starting at 40°C and ending at 55°C in 8 min.

Haloacetonitriles (HANs) were analysed by the 551.1 EPA extraction method followed by GC-MS determination as described elsewhere (Le Roux et al. 2011). Detection limits for DBPs were 0.1 µg L⁻¹.

2.8. Toxicity assessment

An estimation of the (eco)toxicity was done for DTG, DPG and the identified TPs by using the US Environmental Protection Agency Toxicity Estimation Software Tool (TEST) version 4.1, which provides a prediction of the toxicity according to quantitative-structure property relationships (QSAR) by the consensus method, which uses an average value of the calculated toxicities by five different developed QSAR methodologies (Carpinteiro et al. 2017, González-Mariño et al. 2015). Only the oral rat LC₅₀, *Daphnia Magna* LC₅₀ and *Tetrahymena pyriformis* 50% growth inhibition concentration (IGC₅₀) were considered since other ecotoxicological endpoints could not be calculated by the software for most TPs.

Besides the QSAR prediction, a bioluminescent *Vibrio Fisheri* test evaluation of the toxicity of DPG and DTG and different chlorination mixtures was performed according to the standard method NF EN ISO 11348-3 (2009) by using a LumisTox® 300. Details of the procedure are described elsewhere (Tawk et al. 2015).

3. Results and Discussion

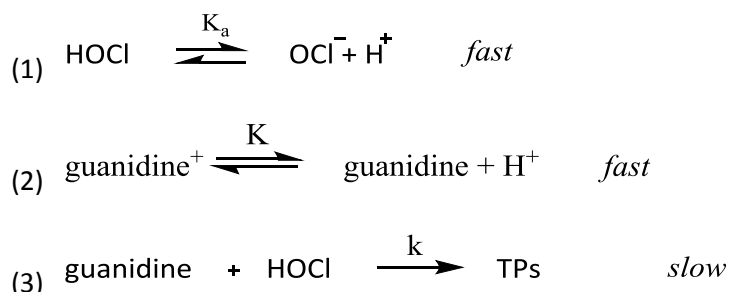
3.1. Chlorination kinetic study

A full kinetic study of DTG and DPG reaction with chlorine was performed considering a wide range of pH from 5 to 11-12. In excess of chlorine, results were adjusted to a pseudo-first order kinetic equation (Figure S1a) to obtain the observed rate constant k_{obs} in s^{-1} as the slope of the linear regression. The first order with respect to chlorine was verified by changing the initial concentration of chlorine (Figure S1b). In addition, it was verified that guanidine concentrations were similar when thiosulfate or ammonium chloride were used to stop the reaction or when manual injection was used without quenching the reaction (Figure S1a) suggesting that N-chlorinated guanidine was not formed (Dodd and Huang 2004).

The apparent rate constant (k_{app} in $M^{-1} s^{-1}$) was determined for each experiment from k_{obs} value and the initial concentration of chlorine. The values of k_{app} are compiled in Tables S1 and S2. They range from $32 M^{-1} s^{-1}$ at pH 5 to a maximum of ca. $1.11 \times 10^4 M^{-1} s^{-1}$ at pH 8.4 for DPG. In the case of DTG, reaction is even faster, with k_{app} ranging from 25 (at pH 4.9, the lowest pH tested in this case) to $1.83 \times 10^4 M^{-1} s^{-1}$ at pH 9.9. At natural water pH values, this translates in very fast reactions, with half-lives of a few seconds to some minutes with typical chlorine doses ($1-10 mg L^{-1}$).

A theoretical model of the pH-dependent apparent rate constant (k_{app}) for the reaction between each guanidine and chlorine was described based on the speciation of HOCl/ ClO^- ($pK_a = 7.54$) and guanidines ($pK_a = 10.67$ for DTG, and $pK_a = 10.12$ for DPG (Perrin 1965)) and considering HOCl as the only active electrophile (Gallard and von Gunten 2002). The large increase in k_{app} when the pH increased from 5 to 9 suggests a

greater contribution of the neutral guanidine to the protonated form. Thus, the resulting model for the DTG and DPG reaction mechanism is described as follows assuming that HOCl reacts only with neutral guanidine species in the first assumption:



The general expression for the reaction of the guanidine compound (either DPG or DTG) with chlorine is then:

$$(4) \quad \frac{d[\text{guanidine}]_T}{dt} = -k[\text{guanidine}][\text{HOCl}] = -k_{app}[\text{guanidine}]_T[\text{HOCl}]_T \quad \textit{and}$$

$$(5) \quad k_{app} = k \alpha_{\text{HOCl}} \alpha_{\text{guanidine}}$$

where: k is the specific rate constant of HOCl with the neutral species of DTG/DPG, K_a is the acid-base equilibrium constant of HOCl, $[\text{HOCl}]_T$ is the total concentration of free chlorine ($\text{HOCl} + \text{OCl}^-$), $[\text{guanidine}]_T$ is the total concentration of DPG or DTG, and α_{HOCl} and $\alpha_{\text{guanidine}}$ are the molar fractions of HOCl and neutral guanidine species, respectively.

By introducing the expression of both, HOCl and guanidine molar fractions, the k_{app} value is given by the following expression:

$$(6) \quad k_{app} = \frac{k K [H^+]}{(K + [H^+])(K_a + [H^+])}$$

The value of the rate constant k was determined by a non-linear least-square regression of the experimental pH profile of the k_{app} values using Sigma Plot 11.0 (Systat Software Inc., San Jose, CA, USA).

The pH dependence of k_{app} is shown in Figures 1a and 1b for DPG and DTG, respectively. For both compounds, the pH profile exhibits a maximum between pH 8 and pH 10. This maximum corresponds to the concomitant presence of both HOCl and neutral guanidine. The maximum pH value is equal to the average value of the pK_a of HOCl and guanidines i.e. 8.8 for DPG and 9.1 for DTG. As shown in Figure 1, the model fits well with the experimental data considering only the reaction of HOCl with neutral guanidine. No improvement was obtained by including the reaction of ClO^- with neutral guanidine and the reaction of HOCl with protonated guanidine (see Text S1 and Table S5), which is in accordance with the literature (Deborde and von Gunten 2002). The rate constants, k , of the reactions between HOCl and DPG and DTG neutral species determined from model fitting to the experimental values are $4.1 (\pm 0.3) \times 10^6 \text{ M}^{-1} \text{ s}^{-1}$ and $2.6 (\pm 0.1) \times 10^7 \text{ M}^{-1} \text{ s}^{-1}$ for DPG and DTG, respectively. The apparent rate constants at neutral pH ($\sim 10^3 \text{ M}^{-1} \text{ s}^{-1}$) and intrinsic rate constants (k) of neutral species ($\sim 10^6 - 10^7 \text{ M}^{-1} \text{ s}^{-1}$) are in the range of rate constants of secondary amines with chlorine (Deborde and von Gunten 2008). However, N-chloroamino compounds were not detected during kinetic experiments and identification of TPs would indicate that initial reactive site is the aromatic ring. Lower rate constant of $19 \text{ M}^{-1} \text{ s}^{-1}$ was obtained for ethyl guanidine at pH 7.2 – 7.4 (Pattison and Davies 2001), which can be explained by the stronger basic character of alkyl guanidines.

3.2. Bromination kinetic study

The apparent rate constants of bromination determined by using direct and competition kinetics methods are listed in Table S3 and S4 for DPG and DTG, respectively and are plotted versus pH in Figure 2. Examples of pseudo-first-order and competition kinetics plots are given in Figure S2 and Figure S3 for DPG. The apparent rate constants range from 76 to $2.89 \times 10^5 \text{ M}^{-1} \text{ s}^{-1}$ for DPG and from 36 to $5.87 \times 10^4 \text{ M}^{-1} \text{ s}^{-1}$ for DTG. In contrast to chlorine, lower rate constants were determined for DTG, which could be attributed to steric effects between the bulky bromine atoms and the methyl groups in DTG.

The experimental results fit well with the proposed model at pHs below 6 and above 9, while a strong deviation and even discrepancies between rate constants determined by the direct kinetics method and the competition kinetics method using BP as reference compound in the pH 7 – 9 range. Such deviations are attributed to a metastable TP with oxidizing properties which could not be identified by LC-HRMS in that pH range (see detailed discussion in Text S2 and Figures S3-S6).

Excluding those pH values, and compared to chlorination, maximum k_{app} values are slightly shifted to higher pH values due to the higher pK_a of HOBr ($\text{pK}_a = 8.8$). Calculated intrinsic rate constants for the reaction of HOBr with neutral DPG and DTG were $8.3 (\pm 0.4) \times 10^6$ and $5.5 (\pm 0.7) \times 10^6$, respectively. While HOBr reacts usually much faster than HOCl with organic compounds (Heeb et al., 2014), the rate constant of HOBr with DPG was only twice as high as the reaction of HOCl with DPG and the rate constant for the reaction of HOBr with DTG was lower than that of HOCl. Steric hindrance (as mentioned), different reactive sites and type of reaction (oxidation vs

substitution) might explain this unexpected result, which requires further investigation.

3.3. Transformation products

Identification of TPs was performed for both DTP and DPG considering chlorination and bromination. Experiments were carried out as described in sections 2.3 and 2.4. All samples were analysed in the LC-QTOF equipment as detailed in 2.6. The proposed structures of the TPs are presented in Figures 3 and 4. Further details on formulas, mass errors and scores of the TPs, as well as individual structures derived from the interpretation of MS/MS spectra are presented in Tables S6 and S7. TPs were named with the precursor compound abbreviation followed by the nominal mass of its $[M+H]^+$ ion. As it can be observed the empirical formula could be proposed with a high degree of certainty, with score values higher than 95% and mass errors lower than 5 ppm, except for DTG-274, whose score was 79% and mass error was 9.7 ppm due to its low intensity.

The proposed structures are based on the interpretation of the MS/MS spectra, which are presented into Figures S7 and S8, for DPG and DTG TPs, respectively. Moreover, DPG-136 (i.e. monophenylguanidine) was unequivocally identified by purchasing its authentic standard from Sigma-Aldrich.

There are four main types of reactions occurring during chlorination, i.e. ipso-chlorination to produce monoguanidine derivatives, introduction of chlorine atoms (bromine when samples are brominated) into an aromatic ring, hydroxylation and intramolecular cyclization. Thus, DPG-136 was easily identified by its spectrum (Figure S7), and because an authentic standard was available, as mentioned. This TP further

reacts by halogenation to the corresponding chlorinated or brominated derivatives (DPG-170 and DPG-214), easily identified because their MS/MS spectra is similar to DPG-136 and exhibit the halogen isotopic pattern (Figure S7). DPG-119 is also produced at long reaction times. Hydroxylation of DPG produces DPG-228, while halogenation produces DPG-246 (chlorination) and DPG-290 (bromination), all of them easily identified by their MS/MS spectra (Figure S7).

A key TP is DPG-210, which a similar empirical formula than DPG itself but with one further double-bond equivalent (i.e. 2 atoms of H less), Table S6. Its MS/MS spectrum exhibits first the loss of ammonia to m/z 192.0671 and also the elimination of CH_3N_2 to m/z 167.0720 from the protonated molecular ion (Figure S7e). This second ion would not be possible unless a cycle is formed. Because of this, we hypothesize here that DPG-210 corresponds to the structure shown in Figure 3, by formation of the 7-membering cycle from DPG-228 (hydroxylated DPG) by elimination of water. In fact the maximum intensity of DPG-228 was observed at 0.5 min and then its intensity rapidly drops, while DPG-210 maximum is reached at 1 min and then drops more slowly (see Figure S9a). The fact that DPG-210 has also been observed as a photolysis TP by Zahn et al. (Zahn et al. 2019), although no structure was proposed in that publication, further supports this hypothesis. Once DPG-210 is formed, this molecule further reacts to yield a mono-hydroxylated-TP (DPG-226), a hydroxychloro-TP (DPG-260) or a dichloro,hydroxy-TP (DPG-294).

In the case of DTG, the reaction was similar to DPG, as expected, but a larger number of TPs could be identified (23 vs. 11 TPs). In general, the main difference in the TPs produced is that a greater degree of hydroxylation and halogenation is observed, e.g.

DTG-308 (a dichlorinated derivative of DTG), which can be explained by the electron-donor effect of the methyl group on aromatic ring. Although no MS/MS spectra (Figure S8) was obtained for all TPs, due to the low intensity of some of them, structures compiled into Figure 4 and Table S7 (those TPs without MS/MS data are marked with a * symbol in the Table) were assigned on the basis of the MS/MS spectra (when available) and by analogy to DPG TPs.

As regards of the most relevant TPs, Figures S9b and 10b present the normalized amount of each TP and their precursors for a reaction with 100 μ M chlorine and up to 30 min of contact time. Normalization was performed by using the signal of the original compound (DPG or DTG) as a surrogate to calculate an approximate yield, except for DPG-136, DPG-119, DPG-170, DTG-150, DTG-166, DTG-184 and DTG-228, where monophenyl-guanidine (DPG-136) was used instead, as being considered structurally closer. In the case of DPG (Figure S9), the most intense TP is DPG-136 with a yield of ca. 5% at 0.5-2 min, dropping down to 3% at 30 min. The second most relevant TP is DPG-246 (monochloro-DPG), with a yield of ca. 3% at 0.5-2 min, dropping down to ca. 0.2% at 30 min. It is noteworthy that at 30 min, there was no DPG detectable and the sum of all TPs intensities would approximately represent a 5% yield. This could likely be attributed to the formation of ring-opening products like chloroform with a relatively high yield (see 3.4) and the uncertainty of the semi-quantitative approach, due to the lack of authentic standards for most TPs.

In the case of DTG (Figure S10), the most intense TP is DTG-254 (hydroxylated cyclic product) with a yield of ca. 30% at 0.5-2 min, followed by DTG-290 (hydroxy,chloro-DTG) with a yield of ca. 15% at 0.5-2 min. These two TPs are also the most relevant at

30 min, representing an estimated yield of 4 and 8% respectively. Also, in the case of DTG, the total yield of TPs at 30 min is ca. 20%.

3.4. Disinfection by-products

Subsequently to TPs identification, we investigated the formation potential of classical DBPs (chloroform and HANs). Chloroform was measured as the only trihalomethane that can be formed without bromide and representing the most relevant group of DBPs, while HANs is another important group of DBPs which can be produced from N-containing chemicals, as it is the case of DPG and DTG. Figure S11 shows the molar yields of CHCl_3 and dichloroacetonitrile (DCAN), the only HAN detected, produced from the chlorination of DPG and DTG after 2 day reaction time. Similar yields were obtained for both guanidines. For CHCl_3 , the yield of ca. 25% for a molar guanidine/ Cl_2 ratio of 1:100 is similar to CHCl_3 yields ranging from 10 to 32% already described for hydroxylated and chlorinated aromatic compounds (Gallard and von Gunten 2002). This is consistent with the formation of chloro or/and hydroxy DPG and DTG that further react with chlorine leading to CHCl_3 as end-product after ring cleavage. Among HANs, only DCAN was detected at significant levels and with yields much lower than CHCl_3 . For a ratio of 1:100, molar yields were 4.4% and 2.3% for DPG and DTG, respectively.

3.5. Reaction in real sample matrices

The reactivity of both guanidine compounds was tested by spiking two real matrices (a surface water and a wastewater effluent) with 1 μM (i.e., ca. 200 $\mu\text{g L}^{-1}$) of either DPG or DTG and 10 μM chlorine and the reaction kinetics followed for 20 min (reaction quenched with ascorbic acid) by LC-HRMS.

In the case of the surface water, DPG and DTG reacted rapidly, being below 1% of their initial concentration after 2 min (Figure S12a-b). Conversely, with the effluent wastewater (with a higher TOC), still an 87% of DPG and 73% of DTG remained after 20 min (Figure S12c-d). Indeed, formation of TPs is easier to happen during drinking water production than by chlorination of wastewater (after secondary treatment). Even so, the chlorinated wastewater was analysed for the TPs previously identified in ultrapure water and several of them could be detected. The amount of bromide in those samples is very low ($<0.1 \text{ mg L}^{-1}$, see 2.2), therefore no brominated TPs were detected. When excluding those brominated TPs, 6 out of 9 TPs were detected for DPG (DPG-136, DPG-228, DPG-210, DPG-226, DPG-260 and DPG-294) and 7 out of 16 were detected for DTG (DTG-150, DTG-256, DTG-290, DTG-239, DTG-254, DTG-270 and DTG-288).

3.6. (Eco)toxicity assessment

To obtain a preliminary estimation of the ecotoxicological implications of the chlorination reaction, the US-EPA TEST software was used in order to predict the toxicity of the two guanidines and their TPs. This prediction was performed only for *Daphnia Magna* LC_{50} (48 h), *Tetrahymena Pyriformis* LC_{50} (48 h) and oral rat LD_{50} (as a proxy of human toxicity), since the software was unable to produce an estimation for other endpoints. The results obtained are summarized in Tables 1 and 2.

As it can be appreciated, oral rat toxicity LD_{50} values are in the $602\text{-}805 \text{ mg Kg}^{-1} \text{ bw}$ for the two guanidines, which would classify them as Category 4 (i.e. the less toxic category) according to the ECHA Guidance (ECHA 2017). The TPs would also be classified as Category 4. Hence human toxicological hazard is expected to be low.

The predicted acute aquatic toxicity endpoint values lie in the 5-28 mg L⁻¹ and 3-6 mg L⁻¹ ranges, for DPG and DTG respectively (Tables 1 and 2). Thus, they would not be classified as Category Acute 1 (the only acute aquatic toxicity category) according to the ECHA Guidance (ECHA 2017). As regards the TPs, the predicted aquatic toxicity of the monoguanidine TPs is lower than the precursor guanidines for the crustacean *Daphnia Magna*, while it could not be predicted for the fish *T. pyriformis*. On the other hand, particularly TPs which are halogenated are predicted to be more toxic. Thus, DPG-294 and 14 TPs from DTG (see Table 1 and 2) would have a predicted toxicity endpoint <1 mg L⁻¹ and would thus be classified in the Category Acute 1 for aquatic organisms. Care must be taken with these data, since the third trophic level (algae) toxicity could not be predicted and values obtained for algae can likely result into more ecotoxicity. In fact DTG is classified in the REACH dossier as Aquatic Acute 1 (ECHA 2018a).

Furthermore, the acute toxicity of DPG and DTG was assessed using the bioluminescent *Vibrio fischeri* test.

The EC₅₀ and EC₂₀ values of *Vibrio fischeri* test were estimated from a series of geometrical dilutions with dilution factors from 1 to 256 and initial guanidine concentration of 100 mg L⁻¹. Figure S13 shows two dose-response curves of DPG after an incubation time of 30 min at 15°C. The initial EC₂₀ of DPG was 40 ±2 mg L⁻¹ and the EC₅₀ was estimated (as detailed in Text S3) to be 245 ±33 mg L⁻¹ from extrapolation of the dose-response curves. The toxicity of DTG was lower and only an EC₂₀ of 80 mg L⁻¹ could be determined. These results confirm that both guanidines have a low acute aquatic toxicity. Due to solubility limitations, the effect of chlorination on acute toxicity

was only tested with a DPG solution of 40 mg L⁻¹ corresponding to the EC₂₀. Chlorination was performed with chlorine doses of 40 and 400 mg Cl₂ L⁻¹ (i.e. molar Cl₂/DPG ratio of 3 and 30). Toxicity tests were conducted after the absence of chlorine residual was checked. Results in Figure 5 shows that the bioluminescence inhibition strongly increases from 14% before chlorination to 45 and 99% for Cl₂/DPG ratios of 3 and 30, respectively. Similar results were generally observed in the literature after chlorination and were assigned to more toxic halogenated TPs (El Najjar et al. 2013, Tawk et al. 2015). Even though the increase of toxicity could not be assigned to specific TPs/DBPs, results of bioluminescent *Vibrio fischeri* test were in agreement with predicted aquatic toxicity endpoints obtained by QSAR.

4. Conclusions

DPG and DTG rapidly react with chlorine and bromine at natural water pH values. This reaction leads to the formation of several TPs via ipso-halogenation, hydroxylation, halogenation and cyclization. Several of these TPs are predicted to be more toxic than the original guanidine compounds, which was confirmed by measuring the acute toxicity of a chlorinated mixture by a *Vibrio Fisheri* acute toxicity assay. Moreover, chlorination leads to the production of the traditional/regulated DBPs chloroform and, to a minor extent, dichloroacetonitrile, when the molar ratio of chlorine to DPG/DTG is high.

Declaration of interests

The authors declare that they have no known competing financial interests or personal relationships that could have appeared to influence the work reported in this paper.

The authors declare the following financial interests/personal relationships which may be considered as potential competing interests:

Acknowledgements

This work was supported by the Water Challenges for a Changing World Joint Program Initiative (Water JPI) Pilot Call (ref. WATERJPI2013 – PROMOTE), funded by the Spanish Ministry of Economy and Competitiveness/Spanish Agencia Estatal de Investigación (refs. JPIW2013-117 and CTM2017-84763-C3-2-R) and French Office National de l'Eau et des Milieux Aquatiques (ref. PROMOTE). We also acknowledge the Galician Council of Culture, Education and Universities (ref. ED431C2017/36), Région Nouvelle Aquitaine and FEDER/EDRF funding.

REFERENCES

Acero, J.L., Benitez, F.J., Real, F.J., Roldan, G. and Rodriguez, E. (2013) Chlorination and bromination kinetics of emerging contaminants in aqueous systems. *Chemical Engineering Journal* 219, 43-50.

Benitez, F.J., Acero, J.L., Real, F.J., Roldan, G. and Casas, F. (2011) Bromination of selected pharmaceuticals in water matrices. *Chemosphere* 85(9), 1430-1437.

Carpinteiro, I., Rodil, R., Quintana, J.B. and Cela, R. (2017) Reaction of diazepam and related benzodiazepines with chlorine. Kinetics, transformation products and in-silico toxicological assessment. *Water Research* 120, 280-289.

Clesceri, L.S., Greenberg, A.E. and Eaton, A.D. (eds) (1998) *Standard Methods for the Examination of Water and Wastewater*, American Water Works Association, Baltimore, MD.

Deborde, M. and von Gunten, U. (2008) Reactions of chlorine with inorganic and organic compounds during water treatment - Kinetics and mechanisms: A critical review. *Water Research* 42(1-2), 13-51.

Dodd, M.C. and Huang, C.H. (2004) Transformation of the antibacterial agent sulfamethoxazole in reactions with chlorine: Kinetics, mechanisms, and pathways. *Environmental Science and Technology* 38(21), 5607-5615.

ECHA (2017) Guidance on the Application of the CLP Criteria. Guidance to Regulation (EC) No 1272/2008 on classification, labelling and packaging (CLP) of substances and mixtures. Version 5.0. July 2017. Agency, E.C. (ed), European Chemicals Agency, Helsinki, Finland.

ECHA (2018a) 1,3-di-o-tolylguanidine (EC number: 202-577-6 | CAS number: 97-39-2) REACH dossier, European Chemicals Agency.

ECHA (2018b) 1,3-diphenylguanidine (EC number: 203-002-1 | CAS number: 102-06-7) REACH dossier, European Chemicals Agency.

El Najjar, N.H., Deborde, M., Journel, R. and Vel Leitner, N.K. (2013) Aqueous chlorination of levofloxacin: Kinetic and mechanistic study, transformation product identification and toxicity. *Water Research* 47(1), 121-129.

Gallard, H. and von Gunten, U. (2002) Chlorination of Phenols: Kinetics and Formation of Chloroform. *Environmental Science & Technology* 36(5), 884-890.

González-Mariño, I., Quintana, J.B., Rodríguez, I., Cores, M. and Cela, R. (2015) Transformation of methadone and its main human metabolite, 2-ethylidene-1,5-dimethyl-3,3-diphenylpyrrolidine (EDDP), during water chlorination. *Water Research* 68, 759-770.

Hernández, F., Ibá, M., Portolés, T., Cervera, M.I., Sancho, J.V. and López, F.J. (2015) Advancing towards universal screening for organic pollutants in waters. *Journal of Hazardous Materials* 282, 86-95.

Hübner, D., Zahn, D., Huppertsberg, S. and Knepper, T.P. (2019) Tires and tire wear particles as source of 1,3-diphenylguanidine and other organic micropollutants in the aquatic environment, Erfurt (Germany).

Jaramillo-loranca, B.E. and Es-ram, L.G. (2015) The Sigma Agonist 1,3-Di-o-tolyl-guanidine Reduces the Morphological and Behavioral Changes Induced by Neonatal Ventral Hippocampus Lesion in Rats. *Synapse* 225(February), 213-225.

Johnson, M. and Melbourne, P. (1996) Photolytic spectroscopic quantification of residual chlorine in potable waters. *Analyst* 121(8), 1075-1078.

Lamy, C., Scuvée-Moreau, J., Dilly, S., Liégeois, J.F. and Seutin, V. (2010) The sigma agonist 1,3-di-o-tolyl-guanidine directly blocks SK channels in dopaminergic neurons and in cell lines. *European Journal of Pharmacology* 641(1), 23-28.

Le Roux, J., Gallard, H. and Croué, J.-P. (2011) Chloramination of nitrogenous contaminants (pharmaceuticals and pesticides): NDMA and halogenated DBPs formation. *Water Research* 45(10), 3164-3174.

Metcalfe, C.D., Miao, X.S., Koenig, B.G. and Struger, J. (2003) Distribution of acidic and neutral drugs in surface waters near sewage treatment plants in the lower Great Lakes, Canada. *Environmental Toxicology And Chemistry* 22(12), 2881-2889.

Montes, R., Aguirre, J., Vidal, X., Rodil, R., Cela, R. and Quintana, J.B. (2017) Screening for Polar Chemicals in Water by Trifunctional Mixed-Mode Liquid Chromatography–High Resolution Mass Spectrometry. *Environmental Science & Technology* 51(11), 6250-6259.

Montes, R., Rodil, R., Cela, R. and Quintana, J.B. (2019) Determination of persistent and mobile organic contaminants (PMOCs) in water samples by mixed-mode liquid chromatography-tandem mass spectrometry. *Analytical Chemistry* 91(8), 5176-5183.

Pattison, D.I. and Davies, M.J. (2001) Absolute Rate Constants for the Reaction of Hypochlorous Acid with Protein Side Chains and Peptide Bonds. *Chemical Research in Toxicology* 14(10), 1453-1464.

Perrin, D.D. (1965) Dissociation constants of organic bases in aqueous solution, IUPAC Publications, London, Butterworths.

Postigo, C. and Richardson, S.D. (2014) Transformation of pharmaceuticals during oxidation/disinfection processes in drinking water treatment. *Journal of Hazardous Materials* 279, 461-475.

Quintana, J.B., Rodil, R. and Rodríguez, I. (2014) Transformation Products of Emerging Contaminants in the Environment. IN: Lambropoulou, D.A. and Nollet, L.M.L. (eds), pp. 123-160, John Wiley and Sons Ltd.

Reemtsma, T., Berger, U., Arp, H.P.H., Gallard, H., Knepper, T.P., Neumann, M., Quintana, J.B. and Voogt, P.D. (2016) Mind the Gap: Persistent and Mobile Organic Compounds - Water Contaminants That Slip Through. *Environmental Science & Technology* 50(19), 10308-10315.

Rodil, R., Quintana, J.B. and Cela, R. (2012) Transformation of phenazone-type drugs during chlorination. *Water Research* 46(7), 2457–2468.

Schulze, S., Zahn, D., Montes, R., Rodil, R., Quintana, J.B., Knepper, T.P., Reemtsma, T. and Berger, U. (2019) Occurrence of emerging persistent and mobile organic contaminants in European water samples. *Water Research* 153, 80-90.

Tang, J., Tang, L., Zhang, C., Zeng, G., Deng, Y., Dong, H., Wang, J. and Wu, Y. (2015) Different senescent HDPE pipe-risk: brief field investigation from source water to tap water in China (Changsha City). *Environmental Science and Pollution Research* 22(20), 16210-16214.

Tawk, A., Deborde, M., Labanowski, J. and Gallard, H. (2015) Chlorination of the β -triketone herbicides tembotrione and sulcotrione: Kinetic and mechanistic study, transformation products identification and toxicity. *Water Research* 76, 132-142.

Zahn, D., Mucha, P., Zilles, V., Touffet, A., Gallard, H., Knepper, T.P. and Frömel, T.

(2019) Identification of potentially mobile and persistent transformation products of

REACH-registered chemicals and their occurrence in surface waters. Water Research

150, 86-96.

Journal Pre-proof

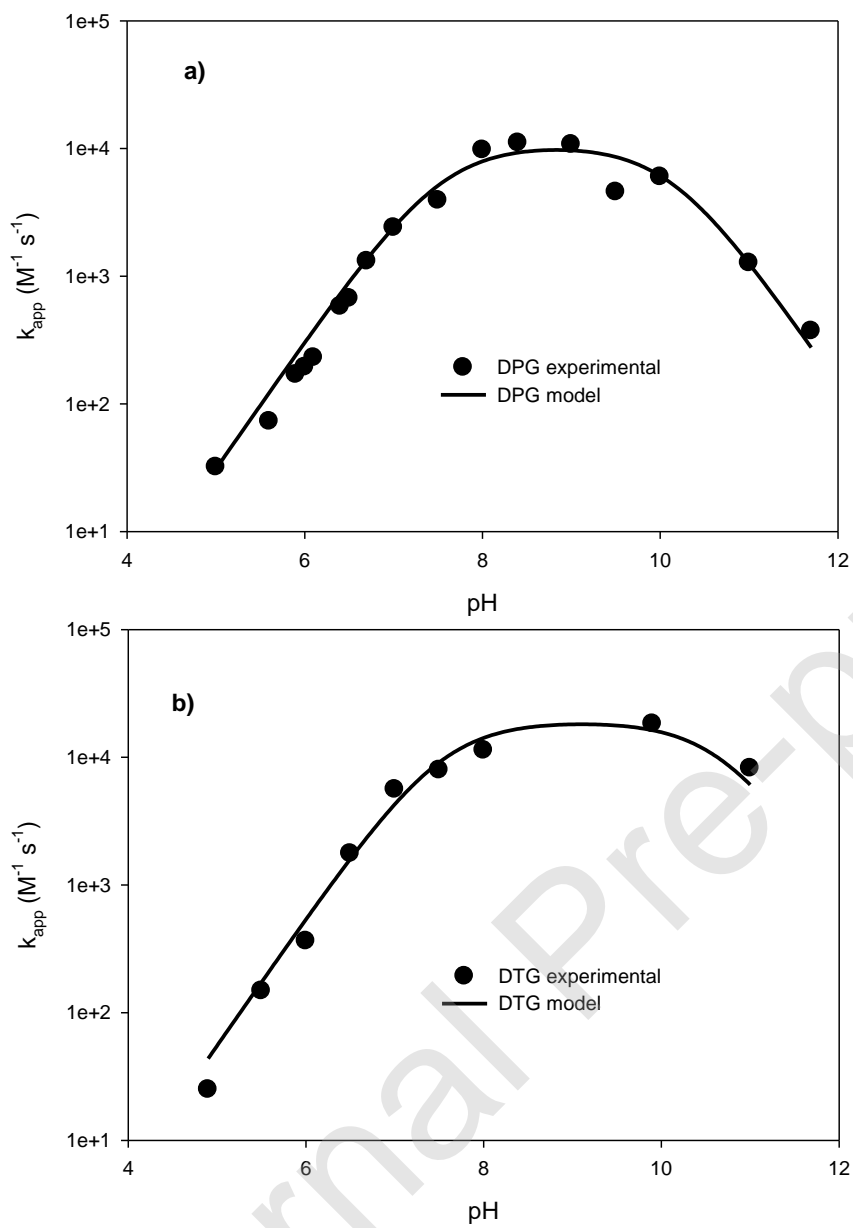


Figure 1. pH dependence of the experimental and modelled apparent rate constants of chlorination of (a) DPG and (b) DTG.

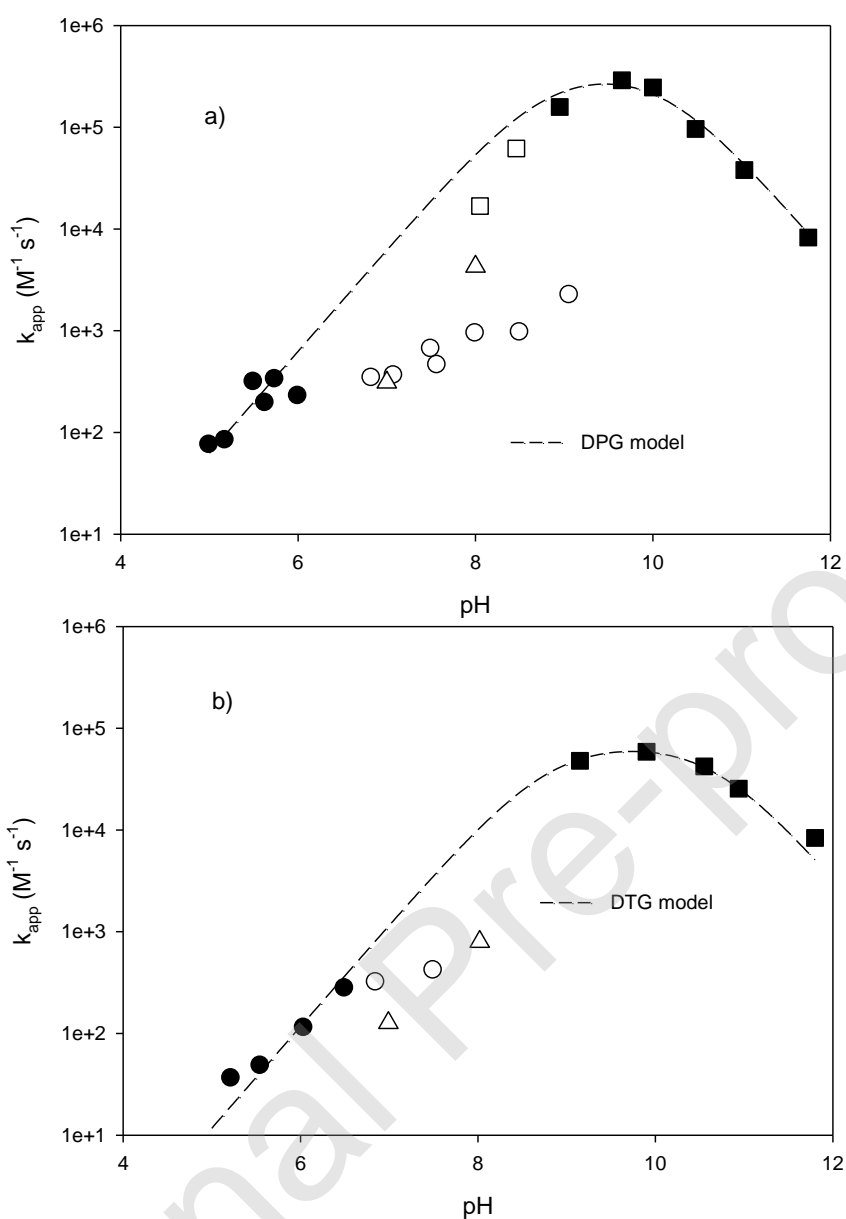


Figure 2. pH dependence of the experimental (symbols) and modelled apparent rate constants of bromination of (a) DPG and (b) DTG. Direct kinetic method (circle) and competitive kinetic method using 4-bromophenol (square) or 2,4,6-tribromophenol (triangle) as reference compounds were used for k_{app} determination. Only full symbols were used for model calculation.

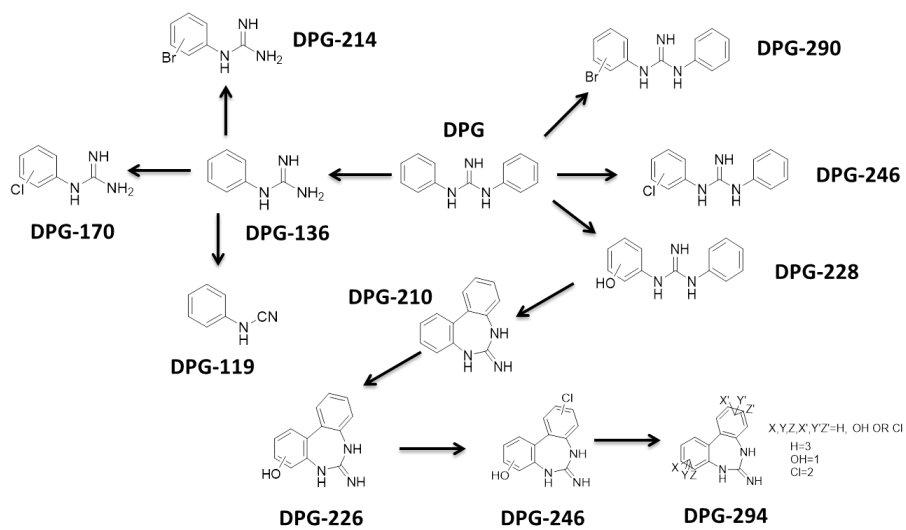


Figure 3. Schematic representation of DPG TPs

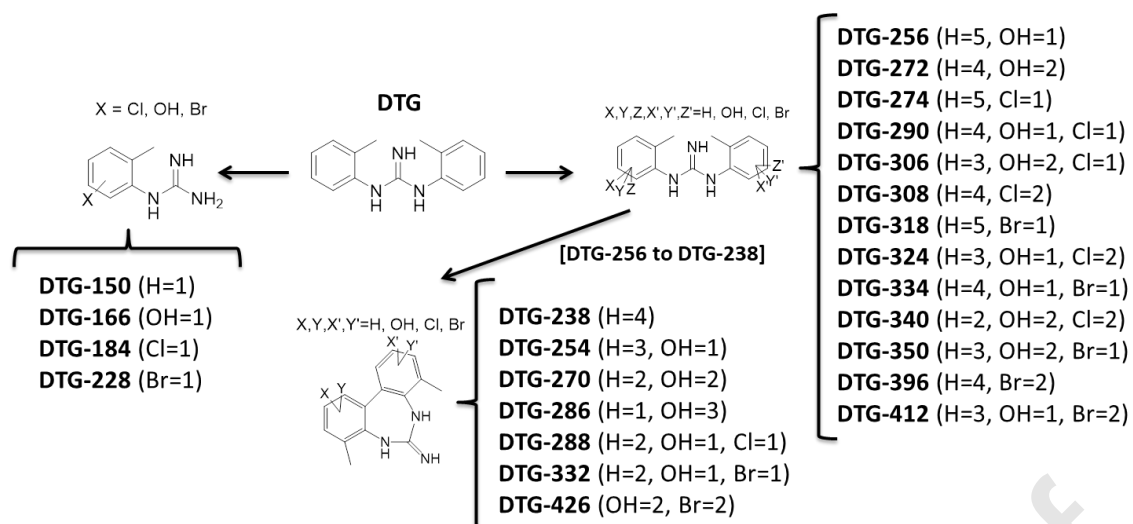


Figure 4. Schematic representation of DTG TPs

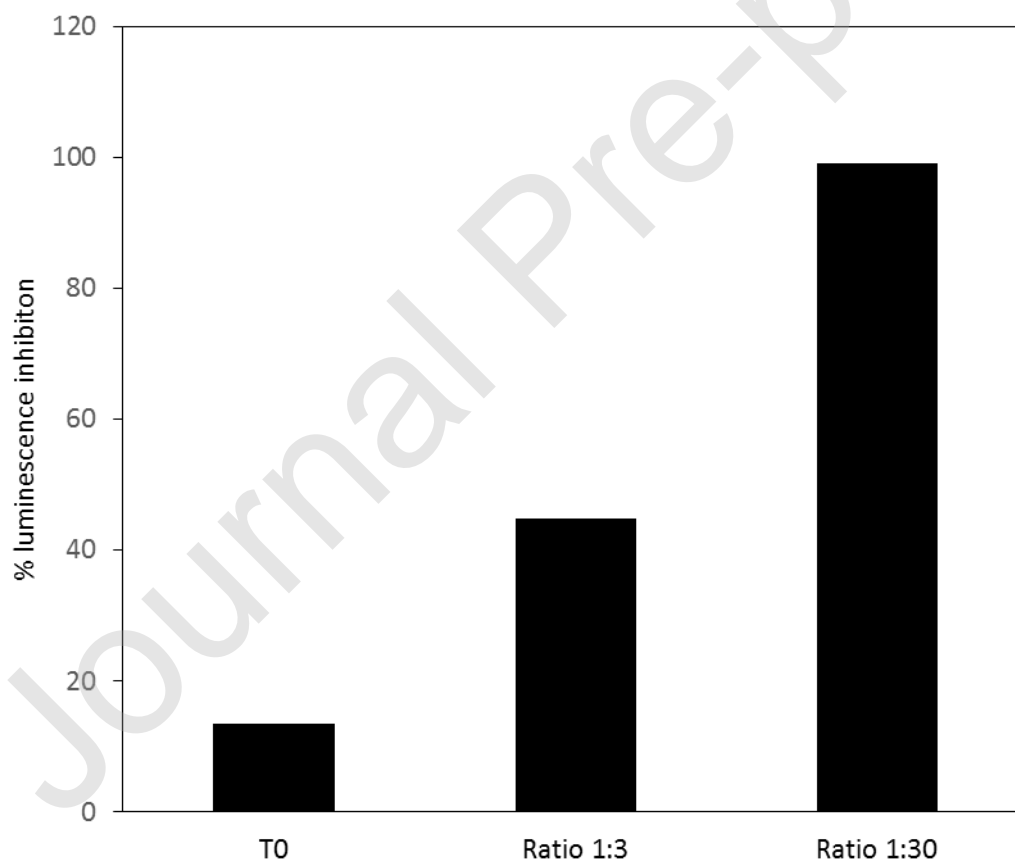


Figure 5. Evolution of bioluminescence inhibition measured using *Vibrio fischeri* Microtox® test during DPG chlorination. $[DPG]_0 = 40 \text{ mg Cl}_2 \text{ L}^{-1}$, molar DPG:Cl₂ ratios of 1:3 and 1:30, chlorination time of 4 days at pH 7.0.

Journal Pre-proof

LIST OF TABLES

Table 1. QSAR Predicted toxicity values for DPG and its TPs.

| | <i>Daphnia magna</i> | <i>T. pyriformis</i> | Oral rat |
|----------------|---------------------------------|----------------------------------|--------------------------|
| | LC ₅₀ (48 hr) (mg/L) | IGC ₅₀ (48 hr) (mg/L) | LD ₅₀ (mg/kg) |
| DPG | 5.09 | 28.5 | 805 |
| DPG-119 | 16.4 | np | 493 |
| DPG-136 | 30.6 | np | 500 |
| DPG-170 | 11.5 | np | 455 |
| DPG-210 | 5.29 | 11.4 | 908 |
| DPG-214 | 1.14 | 9.53 | 1320 |
| DPG-226 | 2.46 | 10.4 | 1143 |
| DPG-228 | 5.24 | 21.1 | 2433 |
| DPG-246 | 1.22 | 7.21 | 886 |
| DPG-260 | 1.89 | 4.78 | 1241 |
| DPG-290 | 1.14 | 9.53 | 1320 |
| DPG-294 | 0.75 | 2.88 | 1019 |

np: no prediction possible

Table 2. QSAR Predicted toxicity values for DTG and its TPs.

| | <i>Daphnia magna</i> | <i>T. pyriformis</i> | Oral rat |
|----------------|---------------------------------|----------------------------------|--------------------------|
| | LC ₅₀ (48 hr) (mg/L) | IGC ₅₀ (48 hr) (mg/L) | LD ₅₀ (mg/kg) |
| DTG | 2.92 | 5.53 | 602 |
| DTG-150 | 27.5 | np | 498 |
| DTG-166 | 23.5 | np | 993 |
| DTG-184 | 22.7 | np | 429 |
| DTG-228 | 5.00 | np | 519 |
| DTG-238 | 3.14 | 6.35 | 553 |
| DTG-254 | 1.68 | 8.26 | 1036 |
| DTG-256 | 3.43 | 9.19 | 1259 |
| DTG-270 | 2.16 | 6.52 | 1121 |
| DTG-272 | 2.52 | 11.2 | 2352 |
| DTG-274 | 0.70 | 2.29 | 1178 |
| DTG-286 | 8.28 | 9.80 | 527 |
| DTG-288 | 0.76 | 1.98 | 721 |
| DTG-290 | 0.93 | 2.14 | 1014 |
| DTG-306 | 0.95 | 2.06 | 1870 |
| DTG-308 | 0.49 | 1.24 | 1109 |
| DTG-318 | 0.39 | 4.35 | 1103 |
| DTG-324 | 0.74 | 1.11 | 940 |
| DTG-332 | 0.51 | 1.55 | 1627 |
| DTG-334 | 0.87 | 3.21 | 927 |
| DTG-340 | 0.31 | 1.11 | 1074 |
| DTG-250 | 0.79 | 2.38 | 1485 |
| DTG-396 | 0.19 | 1.46 | 563 |
| DTG-412 | 0.28 | 1.21 | 823 |
| DTG-426 | 0.03 | 0.55 | 384 |

np: no prediction possible

SUPPORTING INFORMATION TO:

CHLORINATION AND BROMINATION OF 1,3-DIPHENYLGUANIDINE AND 1,3-DI-O-TOLYLGUANIDINE: KINETICS, TRANSFORMATION PRODUCTS AND TOXICITY ASSESSMENT

Benigno J. Sieira ¹, Rosa Montes ¹, Arnaud Touffet ², Rosario Rodil ¹, Rafael Cela ¹, Hervé Gallard ^{2*}, José Benito Quintana ^{1*}

¹ Department of Analytical Chemistry, Nutrition and Food Sciences, Institute of Food Analysis and Research (IIAA), Universidade de Santiago de Compostela, R/ Constantino Candeira S/N, 15782 – Santiago de Compostela (Spain)

² Institut de Chimie des Milieux et des Matériaux de Poitiers (IC2MP) UMR CNRS 7285, École Nationale Supérieure d'Ingénieurs de Poitiers (ENSIP), Université de Poitiers, 1, rue Marcel Doré, TSA 41105, 86073 – Poitiers (France)

* Corresponding authors:

Hervé Gallard: herve.gallard@univ-poitiers.fr

José Benito Quintana: jb.quintana@usc.es

TABLE OF CONTENTS:

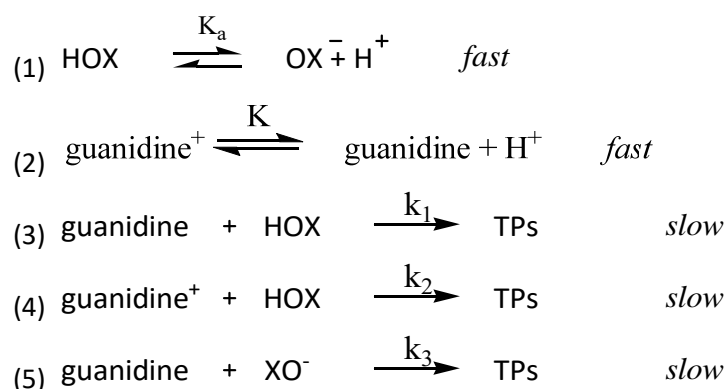
| CONTENT | Page |
|--|-------------|
| Text S1. Full kinetic model | 5 |
| Text S2. Further experiments investigating guanidines bromination | 7 |
| Text S3. Description of Microtox® test inhibition calculations. | 9 |
| Table S1. Experimentally obtained k_{app} for DPG at the different pH values and corresponding half-lives calculated for 10 μM Cl_2 (i.e. 0.71 mg $\text{Cl}_2 \text{L}^{-1}$). | 10 |
| Table S2. Experimentally obtained k_{app} for DTG at the different pH values and corresponding half-lives calculated for 10 μM Cl_2 (i.e. 0.71 mg $\text{Cl}_2 \text{L}^{-1}$). | 11 |
| Table S3. Experimentally obtained k_{app} , kinetics methods for bromination of DPG at the different pH values and corresponding half-lives calculated for 10 μM Br_2 (i.e. 0.71 mg $\text{Br}_2 \text{L}^{-1}$). BP and TBP are 4-bromophenol and 2,4,6-tribromophenol, respectively. Values of k_{ref} are apparent rate constants of BP and TBP calculated from Heeb et al. (2014). | 12 |
| Table S4. Experimentally obtained k_{app} , kinetics methods for bromination of DTG at the different pH values and corresponding half-lives calculated for 10 μM Br_2 (i.e. 0.71 mg $\text{Br}_2 \text{L}^{-1}$). BP and TBP are 4-bromophenol and 2,4,6-tribromophenol, respectively. Values of k_{ref} are apparent rate constants of BP and TBP calculated from Heeb et al. (2014). | 13 |
| Table S5. Specific rate constants of halogenation of DPG and DTG determined by kinetic modelling considering simple or full kinetic model. | 14 |
| Table S6. List of chlorination and bromination DPG TPs. | 15 |
| Table S7. List of chlorination and bromination DTG TPs. | 17 |
| Figure S1. Examples of pseudo-first-order kinetics plots obtained during the chlorination of DPG (Phosphate buffer 10 mM). (a) Influence of pH and quenching methods ($[\text{DPG}]_0$ 1 μM , $[\text{chlorine}]_0$ 10 μM). The reaction was | 21 |

| | |
|---|-----------|
| <p>stopped by thiosulfate (full circle), ammonium (open circle) or manual direct injection was used (open square). Linear regressions are plotted for reduction by thiosulfate. (b) Influence of chlorine concentrations ($[DPG]_0$ 1 μM, pH 6.1). The reaction was stopped by thiosulfate.</p> | |
| <p>Figure S2. Examples of pseudo-first order kinetics plots obtained for bromination of DPG (Phosphate buffer 10 mM). (a) Influence of pH ($[DPG]_0$ 1 μM). The reaction was stopped by thiosulfate. (b) Influence of bromine concentration and quenching method ($[DPG]_0$ 1 μM, pH 5.6). The reaction was stopped by thiosulfate (full circle) or manual direct injection was used (open circle). Linear regression is plotted for reduction by thiosulfate.</p> | 22 |
| <p>Figure S3. Determination of apparent second order rate constants for bromination of DPG by using competition kinetics method with (a) 4-bromophenol (BP) and (b) 2,4,6-tribromophenol (TBP) as reference compound ($[DPG]_0$ 5 μM, $[BP]_0$ or $[TBP]_0$ 5 μM, $[bromine]_0$ 0 to 10 μM, phosphate buffer 10 mM)</p> | 23 |
| <p>Figure S4. Determination of apparent rate constant of bromination of TBP (pH 6.94, $[TBP]_0$ 1 μM, $[bromine]_0$ 20 μM, 10 mM phosphate buffer)</p> | 24 |
| <p>Figure S5. Decay of oxidant response during bromination of DPG (pH 6.9, $[DPG]_0$ 50 μM, $[bromine]_0$ 5 μM, phosphate buffer 10 mM)</p> | 25 |
| <p>Figure S6. UV/visible spectra of DPG solution before and after bromine addition (pH 6.9, 10 mM phosphate buffer, $[DPG]_0$ 50 μM, $[Br_2]_0$ 50 μM, reduction by an excess of thiosulfate)</p> | 25 |
| <p>Figure S7. Chromatograms and MS/MS spectra of DPG and its TPs.</p> | 26 |
| <p>Figure S8. Chromatograms and MS/MS spectra of DTG and its TPs.</p> | 38 |
| <p>Figure S9. Plot summarizing the formation of TPs from DPG (10 μM DPG + 100 μM Cl_2) at different reaction times: (a) results normalized to the time when the TP reached its maximum; (b) results normalized by assuming that the response of the TPs was equal to DPG, except for DPG-136, DPG-119 and</p> | |

| | |
|---|-----------|
| DPG-170 (where DPG-136 was used instead) | |
| Figure S10. Plot summarizing the formation of TPs from DTG (10 μM DTG + 100 μM Cl_2) at different reaction times: (a) results normalized to the time when the TP reached its maximum; (b) results normalized by assuming that the response of the TPs was equal to DTG, except for DTG-150, DTG-166, DTG-184 and DTG-228 (where DPG-136 was used instead). | 53 |
| Figure S11. Molar yield of chloroform and dichloroacetonitrile (DCAN) obtained at different molar DPG/DTG:chlorine ratios: (a) DPG, (b) DTG. (pH 7.0, $[\text{DPG}]_0$ or $[\text{DTG}]_0 = 10 \mu\text{M}$, reaction time 48 hours). | 54 |
| Figure S12. Dissipation plots during the chlorination of real water samples (1 μM DPG/DTG + 10 μM Cl_2): (a) DPG in river water, (b) DTG in river water, (c) DPG in effluent, (d) DTG in effluent. | 55 |
| Figure S13. Dose-response curves $\log(\text{Ct})$ versus $\log(\text{Ht} / (100 - \text{Ht}))$ for EC_{50} and EC_{20} value calculations of DPG toxicity using Microtox [®] test. See text S1 for calculation details. The two different symbols correspond to two replicate experiments. | 56 |

Text S1. Full kinetic model

A full kinetic model was evaluated for initial reaction of halogenation of guanidines. The model includes the reactions of hypohalous acid (HOCl or HOBr) with neutral or protonated guanidines and the reaction of hypohalite ion (ClO⁻ or BrO⁻) with neutral guanidine:



Then, the general expression for the rate of halogenation of guanidine is given by the following expression

$$(6) \quad \frac{d[\text{guanidine}]_T}{dt} = -k_1 [\text{guanidine}][\text{HOX}] - k_2 [\text{guanidine}^+][\text{HOX}] - k_3 [\text{guanidine}][\text{XO}^-] = -k_{app} [\text{guanidine}]_T [\text{HOX}]_T$$

The apparent rate constant depends on the intrinsic rate constants k_1 , k_2 , and k_3 and the molar fractions of guanidine and halogen species.

$$(7) \quad \text{and } k_{app} = k_1 \alpha_{HOX} \alpha_{\text{guanidine}} + k_2 \alpha_{HOX} \alpha_{\text{guanidine}^+} + k_3 \alpha_{XO^-} \alpha_{\text{guanidine}}$$

Replacing the molar fractions by their expressions in function of H^+ concentration and equilibrium rate constants give the following expression for k_{app} :

$$(8) \quad k_{app} = \frac{k_1 K [\text{H}^+] + k_2 [\text{H}^+]^2 + k_3 K K_a}{(K_a + [\text{H}^+])(K + [\text{H}^+])}$$

Specific rate constants and coefficients of determination obtained by kinetic modelling by non-linear regression (Sigma Plot 11.0) of the experimental pH profile of apparent rate constants are given in Table S5. Values are compared with values obtained by the simple kinetic model considering only the reaction of HOX with neutral guanidine.

The results presented in Table S5 show that, except for chlorination of DTG, values of k_2 and k_3 are very low or equal to zero and that determination coefficients are similar for the two models. The only significant k_3 value of $3.9 \times 10^3 \text{ M}^{-1} \text{ s}^{-1}$ was generated for the chlorination of DTG with slightly higher R^2 for full kinetic model. Still k_3 is 4 orders of magnitude lower than k_1 . This did not justify the use of the full kinetic model in place of the simple model because this result only depends on the unique value of k_{app} at pH 11.0 for DTG.

Text S2. Further experiments investigating guanidines bromination

Several experiments were conducted in order to further investigate the observed deviation from the model during the bromination of DPG and DTG. For DPG, apparent rate constants determined at pH 8.5 and 9.0 by the direct kinetics method in batch reactor were about 70-fold lower than rate constants determined by the competition method using BP as reference compound. These rate constants are even 10-fold lower than rate constants obtained during chlorination for the same pH range. Competition kinetic method using TBP as reference compound (Figure S3b) gave also low apparent constants at pH 7.0 and 8.0 and in the range of rate constants determined by the direct method. Such experimental pH profiles of k_{app} could not be explained by speciation of bromine or guanidines.

A further experiment performed at pH 6.9 with an excess of DPG (50 μ M) compared to bromine (5 μ M) was performed. Residual oxidant was then analysed for different reaction times as triiodide at 351 nm ($\epsilon = 26\ 900\ \text{M}^{-1}\ \text{cm}^{-1}$, Cimetiere et al. (2009)) in a 5-cm quartz spectrophotometric cell after addition of 250 μ L of 1 M KI phosphate buffer (pH 6.5) solution in 5 mL of sample. This experiment showed an strong deviation from the linear form of the pseudo-first-order kinetic model (Figure S5), which suggests that compound(s) with oxidant properties remained in solution and could interfere in rate constant determination.

Finally, when a higher concentration of 50 μ M bromine was added in a 50 μ M DPG solution at pH 6.9, the colourless solution turned pink progressively for 3 minutes and colour disappeared after addition of thiosulfate (see Figure S6 for UV/visible spectra). In absence of thiosulfate, colour slowly disappeared for about 12 hours. The visible absorption band was centered at 520 nm. These observations are very similar to the formation of the highly colored semiquinoid free radical formed during oxidation of N,N-di-ethyl-p-phenylenediamine and commonly used for chlorine analysis (Harp, 2002). Even though phenylguanidines differ from aromatic p-diamines and that the formation of a radical cation during the oxidation of phenylguanidines could not be confirmed in our study, a stable transformation product (TP) with oxidizing property likely affected the determination of rate constants with bromine at pH 7 – 8. Such TP

existence could not be confirmed, however, by LC-HRMS, likely because it is reduced by the chromatographic eluents.

References:

Cimetiere N., Dossier-Berne F., De Laat J. (2009) Monochloramination of resorcinol: mechanism and kinetic modelling. *Environmental Science and Technology* 43, 9380 - 9385.

Harp, D.L. (2002). *Current Technology of Chlorine Analysis for Water and Wastewater*. Technical Information Series--Booklet No 17.

Text S3. Description of Microtox® test inhibition calculations.

The inhibition of the luminescence was calculated according to the following equation:

$$H_t = \frac{I_{ct} - I_t}{I_{ct}} \times 100$$

where H_t is the inhibition percentage of the luminescence after the incubation period t ,

I_t is the luminescence of the test solutions after the 30 min incubation period (i.e. the final luminescence after addition of the sample),

I_{ct} the corrected initial luminescence for the tested solution with $I_{ct} = f_k \times I_o$, and I_o was the initial luminescence of the bacteria suspensions before the sample was added, f_k the correction factor $f_k = \frac{I_{tK}}{I_{oK}}$ with I_{oK} is the initial luminescence of the control solution (2% NaCl) and I_{tK} is the luminescence of the control solution (2% NaCl) after the 30 min incubation period.

The EC_{50} and EC_{20} values were calculated from the linear representation of $\log(c_t)$ versus $\log(H_t/(100 - H_t))$, where $c_t = 100 \times (1/\text{dilution factor})$. The EC_{50} value was given by the point of intersection with the X-axis at $\log(H_t/(100 - H_t)) = 0$. The EC_{20} value was determined for $\log(H_t/(100 - H_t)) = -0.60$.

Table S1. Experimentally obtained k_{app} for DPG at the different pH values and corresponding half-lives calculated for 10 μM Cl_2 (i.e. 0.71 mg Cl_2 L^{-1}).

| pH | k_{app} ($\text{M}^{-1} \text{s}^{-1}$) | $t_{1/2}$ (s) |
|-----------|--|---------------------------------|
| 5.0 | 32 | 2203 |
| 5.6 | 73 | 950 |
| 5.9 | 170 | 408 |
| 6.0 | 194 | 357 |
| 6.1 | 230 | 301 |
| 6.4 | 580 | 120 |
| 6.5 | 670 | 104 |
| 6.7 | 1310 | 53 |
| 7.0 | 2400 | 29 |
| 7.5 | 3923 | 18 |
| 8.0 | 9760 | 7 |
| 8.4 | 11061 | 6 |
| 9.0 | 10776 | 6 |
| 9.5 | 4567 | 15 |
| 10.0 | 5999 | 12 |
| 11.0 | 1269 | 55 |
| 11.7 | 372 | 186 |

Table S2. Experimentally obtained k_{app} for DTG at the different pH values and corresponding half-lives calculated for 10 μM Cl_2 (i.e. 0.71 mg Cl_2 L^{-1}).

| pH | k_{app} ($\text{M}^{-1} \text{s}^{-1}$) | $t_{1/2}$ (s) |
|-----------|--|---------------------------------|
| 4.9 | 25 | 2803 |
| 5.5 | 148 | 469 |
| 6.0 | 364 | 190 |
| 6.5 | 1764 | 39 |
| 7.0 | 5599 | 12 |
| 7.5 | 7941 | 9 |
| 8.0 | 11327 | 6 |
| 9.9 | 18297 | 4 |
| 11.0 | 8205 | 9 |

Table S3. Experimentally obtained k_{app} , kinetics methods for bromination of DPG at the different pH values and corresponding half-lives calculated for 10 μM Br_2 (i.e. 0.71 mg $\text{Br}_2 \text{L}^{-1}$). BP and TBP are 4-bromophenol and 2,4,6-tribromophenol, respectively. Values of k_{ref} are apparent rate constants of BP and TBP calculated from Heeb et al. (2014).

| pH | Kinetic method | k_{ref} ($\text{M}^{-1} \text{s}^{-1}$) | k_{app} ($\text{M}^{-1} \text{s}^{-1}$) | $t_{1/2}$ (s) |
|-------|----------------------|--|--|------------------|
| 5.00 | direct | - | 76 | 916.9 |
| 5.18 | direct | - | 84 | 827.0 |
| 5.50 | direct | - | 314 | 220.7 |
| 5.63 | direct | - | 195 | 354.7 |
| 5.74 | direct | - | 334 | 207.5 |
| 6.00 | direct | - | 228 | 304.0 |
| 6.83 | direct | - | 344 | 201.6 |
| 7.00 | competition with TBP | 2112 | 311 | 222.9 |
| 7.08 | direct | - | 363 | 190.9 |
| 7.57 | direct | - | 460 | 150.7 |
| 8.00 | direct | - | 940 | 73.7 |
| 8.00 | competition with TBP | 2842 | 4276 | 16.2 |
| 8.05 | competition with BP | 26900 | 16829 | 4.1 |
| 8.50 | direct | - | 962 | 72.1 |
| 8.46 | competition with BP | 50700 | 61934 | 1.1 |
| 8.95 | competition with BP | 93300 | 158254 | 0.4 |
| 9.06 | direct | - | 2240 | 30.9 |
| 9.65 | competition with BP | 439000 | 289338 | 0.2 |
| 10.00 | competition with BP | 245910 | 246000 | 0.3 |
| 10.48 | competition with BP | 93300 | 96164 | 0.7 |
| 11.03 | competition with BP | 27700 | 37977 | 1.8 |
| 11.75 | competition with BP | 5360 | 8245 | 8.4 |

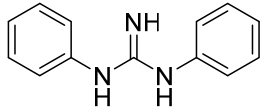
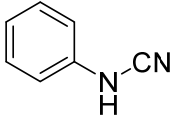
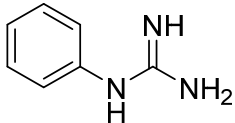
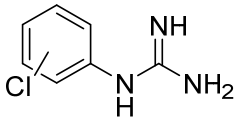
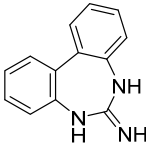
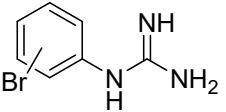
Table S4. Experimentally obtained k_{app} , kinetics methods for bromination of DTG at the different pH values and corresponding half-lives calculated for 10 μM Br_2 (i.e. 0.71 mg $\text{Br}_2 \text{L}^{-1}$). BP and TBP are 4-bromophenol and 2,4,6-tribromophenol, respectively. Values of k_{ref} are apparent rate constants of BP and TBP calculated from Heeb et al. (2014).

| pH | Kinetic method | k_{ref} ($\text{M}^{-1} \text{s}^{-1}$) | k_{app} ($\text{M}^{-1} \text{s}^{-1}$) | $t_{1/2}$ (s) |
|-------|----------------------|--|--|------------------|
| 5.22 | direct | - | 36 | 1918.4 |
| 5.55 | direct | - | 48 | 1438.6 |
| 6.04 | direct | - | 113 | 611.7 |
| 6.50 | direct | - | 277 | 250.3 |
| 6.85 | direct | - | 318 | 217.8 |
| 6.99 | competition with TBP | 2112 | 127 | 545.8 |
| 7.50 | direct | - | 417 | 166.2 |
| 8.02 | competition with TBP | 2842 | 797 | 86.9 |
| 9.15 | competition with BP | 698000 | 47857 | 1.4 |
| 9.90 | competition with BP | 294000 | 58707 | 1.2 |
| 10.55 | competition with BP | 80300 | 42185 | 1.6 |
| 10.94 | competition with BP | 33900 | 25430 | 2.7 |
| 11.80 | competition with BP | 4780 | 8355 | 8.3 |

Table S5. Specific rate constants of halogenation of DPG and DTG determined by kinetic modelling considering simple or full kinetic model.

| | | Full model | | | | Simple model | |
|--------------|-----|-------------------|----------------------|----------------------|-------|-------------------|-------|
| | | k_1 | k_2 | k_3 | R^2 | k | R^2 |
| Chlorination | DPG | 4.1×10^6 | 1.4×10^{-7} | 2.4×10^{-6} | 0.898 | 4.1×10^6 | 0.898 |
| | DTG | 2.4×10^7 | 2.5×10^{-8} | 3.9×10^3 | 0.975 | 2.6×10^7 | 0.960 |
| Bromination | DPG | 8.3×10^6 | 2.2×10^{-8} | 0 | 0.950 | 8.3×10^6 | 0.950 |
| | DTG | 5.5×10^6 | 1.2×10^{-6} | 0 | 0.997 | 5.5×10^6 | 0.997 |

Table S6. List of chlorination and bromination DPG TPs.

| Name | Experimental m/z | Molecular formula | Theoretical m/z | Error (ppm) | Error (mDa) | DBE | Score (%) | Structure |
|---------|------------------|---|-----------------|-------------|-------------|-----|-----------|---|
| DPG | 212.1182 | C ₁₃ H ₁₃ N ₃ | - | - | - | 9 | - |  |
| DPG-119 | 119.0604 | C ₇ H ₆ N ₂ | 119.0604 | - 0.21 | - 0.03 | 6 | 100.00 |  |
| DPG-136 | 136.0867 | C ₇ H ₉ N ₃ | 136.0869 | 1.66 | 0.22 | 5 | 99.69 |  |
| DPG-170 | 170.0475 | C ₇ H ₈ N ₃ Cl | 170.0480 | 2.67 | 0.45 | 5 | 98.90 |  |
| DPG-210 | 210.1025 | C ₁₃ H ₁₁ N ₃ | 210.1026 | 0.35 | 0.07 | 10 | 99.97 |  |
| DPG-214 | 213.9968 | C ₇ H ₈ N ₃ Br | 213.9974 | 2.99 | 0.64 | 5 | 98.14 |  |

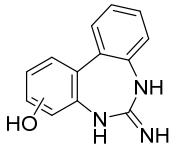
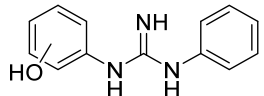
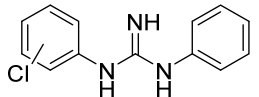
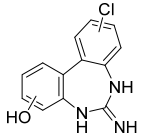
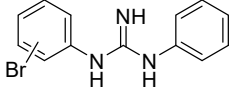
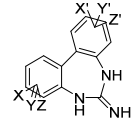
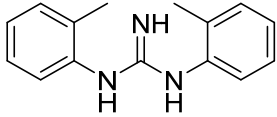
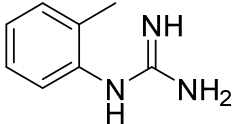
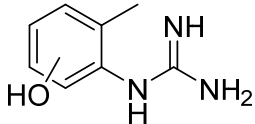
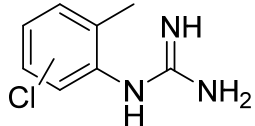
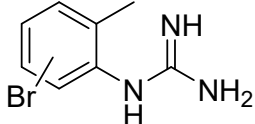
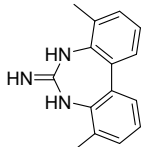
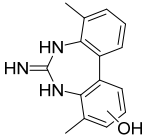
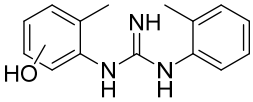
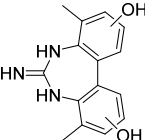
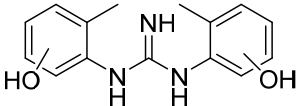
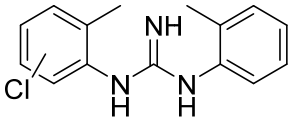
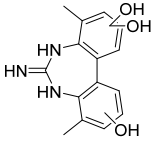
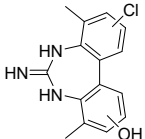
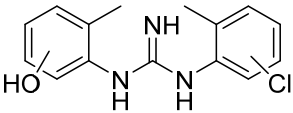
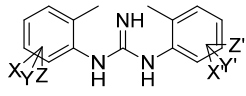
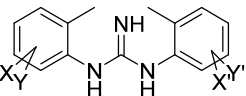
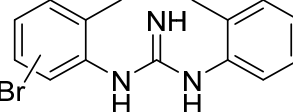
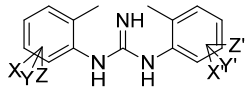
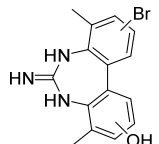
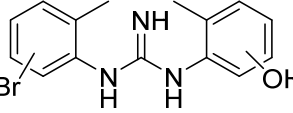
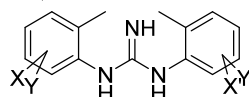
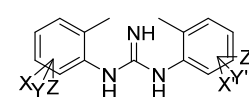
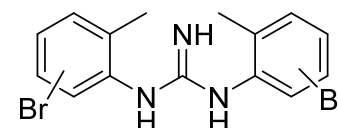
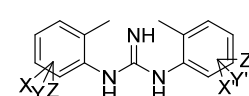
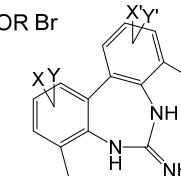
| | | | | | | | | |
|----------------|----------|---|----------|--------|--------|----|--------|---|
| DPG-226 | 226.0975 | C ₁₃ H ₁₁ N ₃ O | 226.0975 | - 0.05 | - 0.01 | 10 | 100.00 |  |
| DPG-228 | 228.1131 | C ₁₃ H ₁₃ N ₃ O | 228.1131 | 0.17 | 0.04 | 9 | 99.99 |  |
| DPG-246 | 246.0795 | C ₁₃ H ₁₂ N ₃ Cl | 246.0793 | - 1.01 | - 0.25 | 9 | 99.74 |  |
| DPG-260 | 260.0579 | C ₁₃ H ₁₀ N ₃ O Cl | 260.0585 | 2.38 | 0.62 | 10 | 98.51 |  |
| DPG-290 | 290.0287 | C ₁₃ H ₁₂ N ₃ Br | 290.0287 | 0.13 | 0.04 | 9 | 100.00 |  |
| DPG-294 | 294.0186 | C ₁₃ H ₉ N ₃ O Cl ₂ | 294.0195 | 3.22 | 0.94 | 10 | 96.91 |  <p>X, Y, Z, X', Y', Z' = H, OH OR Cl H=3 OH=1 Cl=2</p> |

Table S7. List of chlorination and bromination DTG TPs.

| Name | Experimental m/z | Molecular formula | Theoretical m/z | Error (ppm) | Error (mDa) | DBE | Score (%) | Structure |
|---------|------------------|--|-----------------|-------------|-------------|-----|-----------|---|
| DTG | 240.1495 | C ₁₅ H ₁₇ N ₃ | - | - | - | 9 | - |  |
| DTG-150 | 150.1026 | C ₈ H ₁₁ N ₃ | 150.1026 | - 0.18 | - 0.03 | 5 | 100.00 |  |
| DTG-166 | 166.0971 | C ₈ H ₁₁ N ₃ O | 166.0975 | 2.35 | 0.39 | 5 | 99.17 |  |
| DTG-184 | 184.0632 | C ₈ H ₁₀ N ₃ Cl | 184.0636 | 2.19 | 0.40 | 5 | 99.17 |  |
| DTG-228 | 228.0131 | C ₈ H ₁₀ N ₃ Br | 228.0131 | - 0.06 | - 0.01 | 5 | 100.00 |  |
| DTG-238 | 238.1336 | C ₁₅ H ₁₅ N ₃ | 238.1339 | 1.16 | 0.27 | 10 | 99.68 |  |

| | | | | | | | | |
|-----------------|----------|---|----------|--------|--------|----|-------|---|
| DTG-254 | 254.1285 | C ₁₅ H ₁₅ N ₃ O | 254.1288 | 1.14 | 0.29 | 10 | 99.66 |  |
| DTG-256 | 256.1436 | C ₁₅ H ₁₇ N ₃ O | 256.1444 | 3.29 | 0.84 | 9 | 97.23 |  |
| DTG-270* | 270.1238 | C ₁₅ H ₁₅ N ₃ O ₂ | 270.1237 | - 0.36 | - 0.10 | 10 | 99.96 |  |
| DTG-272 | 272.1391 | C ₁₅ H ₁₇ N ₃ O ₂ | 272.1394 | 0.93 | 0.25 | 9 | 99.75 |  |
| DTG-274* | 274.1079 | C ₁₅ H ₁₆ N ₃ Cl | 274.1106 | 9.71 | 2.65 | 9 | 79.46 |  |
| DTG-286* | 286.1182 | C ₁₅ H ₁₅ N ₃ O ₃ | 286.1186 | 1.47 | 0.42 | 10 | 99.36 |  |
| DTG-288* | 288.0895 | C ₁₅ H ₁₄ N ₃ O Cl | 288.0898 | 1.10 | 0.32 | 10 | 99.64 |  |

| | | | | | | | | |
|-----------------|----------|--|----------|--------|--------|----|--------|---|
| DTG-290 | 290.1042 | C ₁₅ H ₁₆ N ₃ O Cl | 290.1055 | 4.38 | 1.27 | 9 | 95.41 |  |
| DTG-306* | 306.0995 | C ₁₅ H ₁₆ N ₃ O ₂ Cl | 306.0931 | 2.89 | 0.88 | 9 | 97.39 | <p>X,Y,Z,X',Y',Z'=H, OH OR Cl</p> <p>H=3 OH=2 Cl=1</p>  |
| DTG-308 | 308.0706 | C ₁₅ H ₁₅ N ₃ Cl ₂ | 308.0716 | 3.19 | 0.98 | 9 | 96.81 | <p>X,Y,X',Y'=H OR Cl</p> <p>H=2 Cl=2</p>  |
| DTG-318 | 318.0600 | C ₁₅ H ₁₆ N ₃ Br | 318.0600 | 0.12 | 0.04 | 9 | 100.00 |  |
| DTG-324 | 324.0657 | C ₁₅ H ₁₅ N ₃ Cl ₂ O | 324.0665 | 2.46 | 0.79 | 9 | 97.98 | <p>X,Y,Z,X',Y',Z'=H, OH OR Cl</p> <p>H=3 OH=1 Cl=2</p>  |
| DTG-332* | 332.0393 | C ₁₅ H ₁₄ N ₃ O Br | 332.0393 | 0.00 | 0.00 | 10 | 100.00 |  |
| DTG-334 | 334.0550 | C ₁₅ H ₁₆ N ₃ O Br | 334.0550 | - 0.15 | - 0.05 | 9 | 99.99 |  |

| | | | | | | | | |
|-----------------|----------|---|----------|--------|--------|----|--------|--|
| DTG-340* | 340.0609 | C ₁₅ H ₁₅ N ₃ O ₂ Cl ₂ | 340.0614 | 1.50 | 0.51 | 9 | 99.20 | <p>X,Y,X',Y'=H, OH OR Cl H=2 Cl=2 OH=2</p>  |
| DTG-350* | 350.0499 | C ₁₅ H ₁₆ N ₃ O ₂ Br | 350.0499 | - 0.10 | - 0.03 | 9 | 100.00 | <p>X,Y,Z,X',Y',Z'=H, OH OR Br H=3 OH=2 Br=1</p>  |
| DTG-396* | 395.9705 | C ₁₅ H ₁₅ N ₃ Br ₂ | 395.9705 | 0.13 | 0.05 | 9 | 99.99 |  |
| DTG-412 | 411.9655 | C ₁₅ H ₁₅ N ₃ O Br ₂ | 411.9655 | - 0.09 | - 0.04 | 9 | 100.00 | <p>X,Y,Z,X',Y',Z'=H, OH OR Br H=3 OH=1 Br=2</p>  |
| DTG-426* | 425.9431 | C ₁₅ H ₁₃ N ₃ O ₂ Br ₂ | 425.9425 | - 1.53 | 1.63 | 10 | 98.97 | <p>X,Y,X',Y'=OH OR Br OH=2 Br=2</p>  |

* TPs with low intensity, thus no MS/MS spectra could be recorded

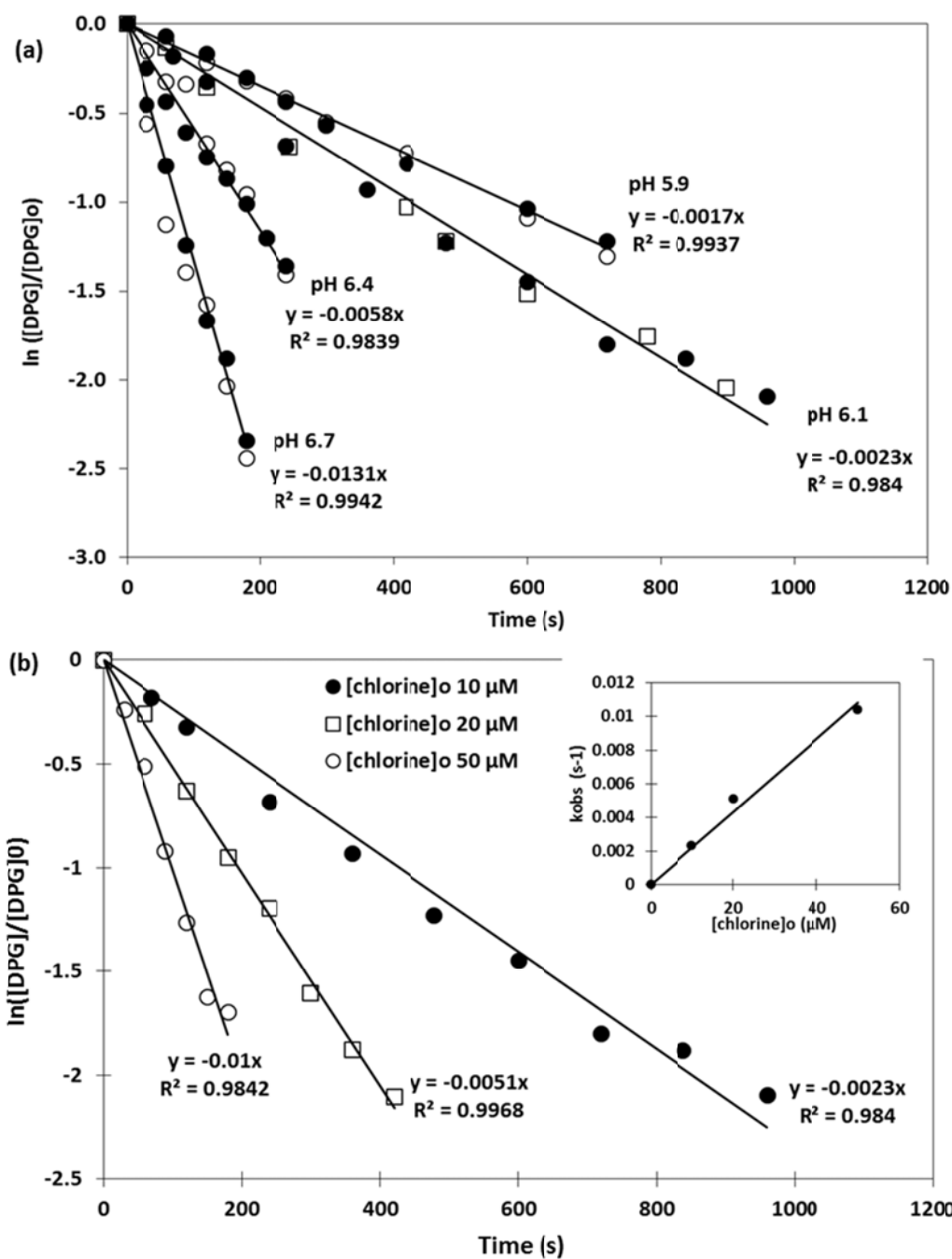


Figure S1. Examples of pseudo-first-order kinetics plots obtained during the chlorination of DPG (Phosphate buffer 10 mM). (a) Influence of pH and quenching methods ($[DPG]_0$ 1 μ M, $[chlorine]_0$ 10 μ M). The reaction was stopped by thiosulfate (full circle), ammonium (open circle) or manual direct injection was used (open square). Linear regressions are plotted for reduction by thiosulfate. (b) Influence of chlorine concentrations ($[DPG]_0$ 1 μ M, pH 6.1). The reaction was stopped by thiosulfate.

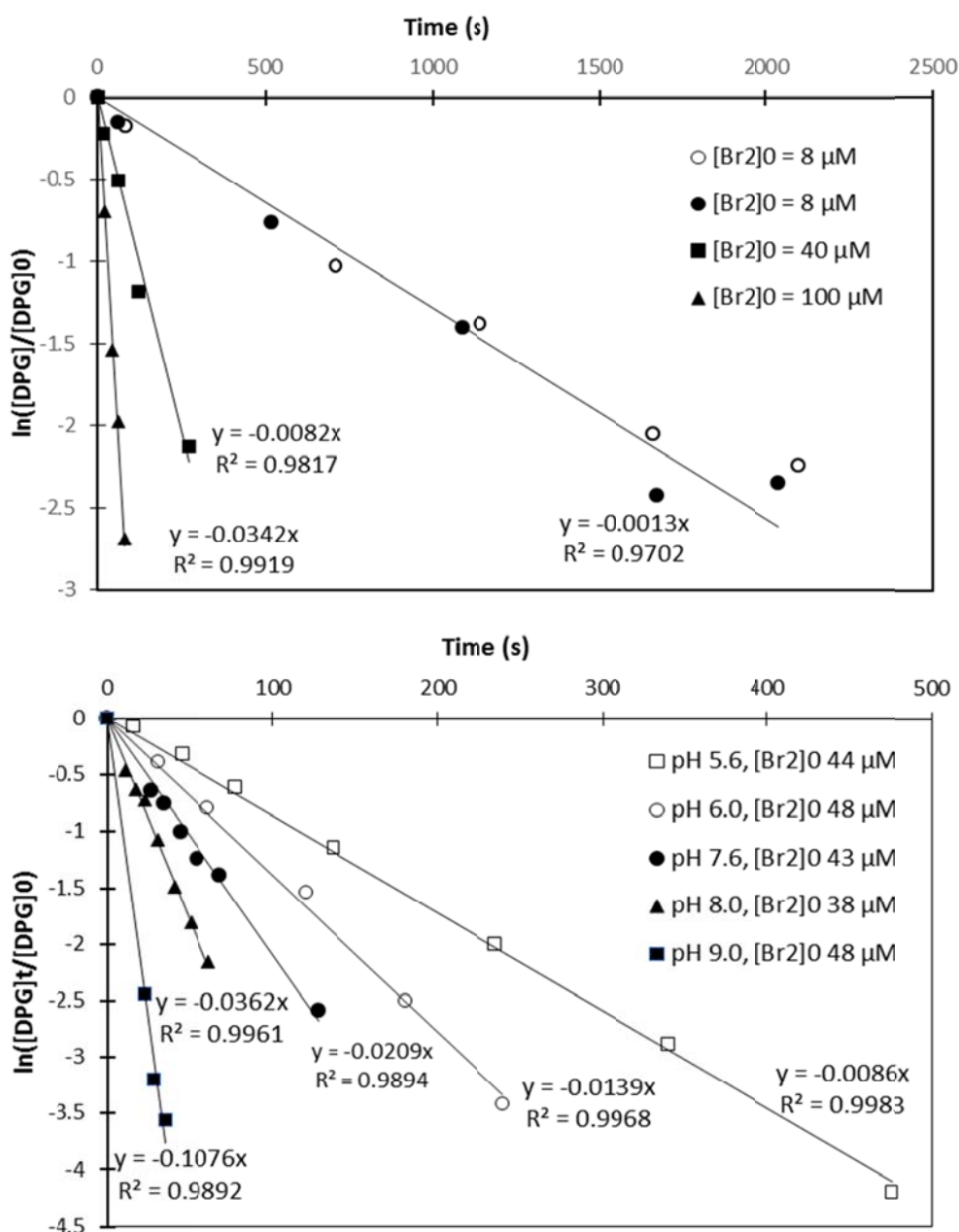


Figure S2. Examples of pseudo-first order kinetics plots obtained for bromination of DPG (Phosphate buffer 10 mM). (a) Influence of pH ($[DPG]_0 = 1 \mu M$). The reaction was stopped by thiosulfate. (b) Influence of bromine concentration and quenching method ($[DPG]_0 = 1 \mu M$, pH 5.6). The reaction was stopped by thiosulfate (full circle) or manual direct injection was used (open circle). Linear regression is plotted for reduction by thiosulfate.

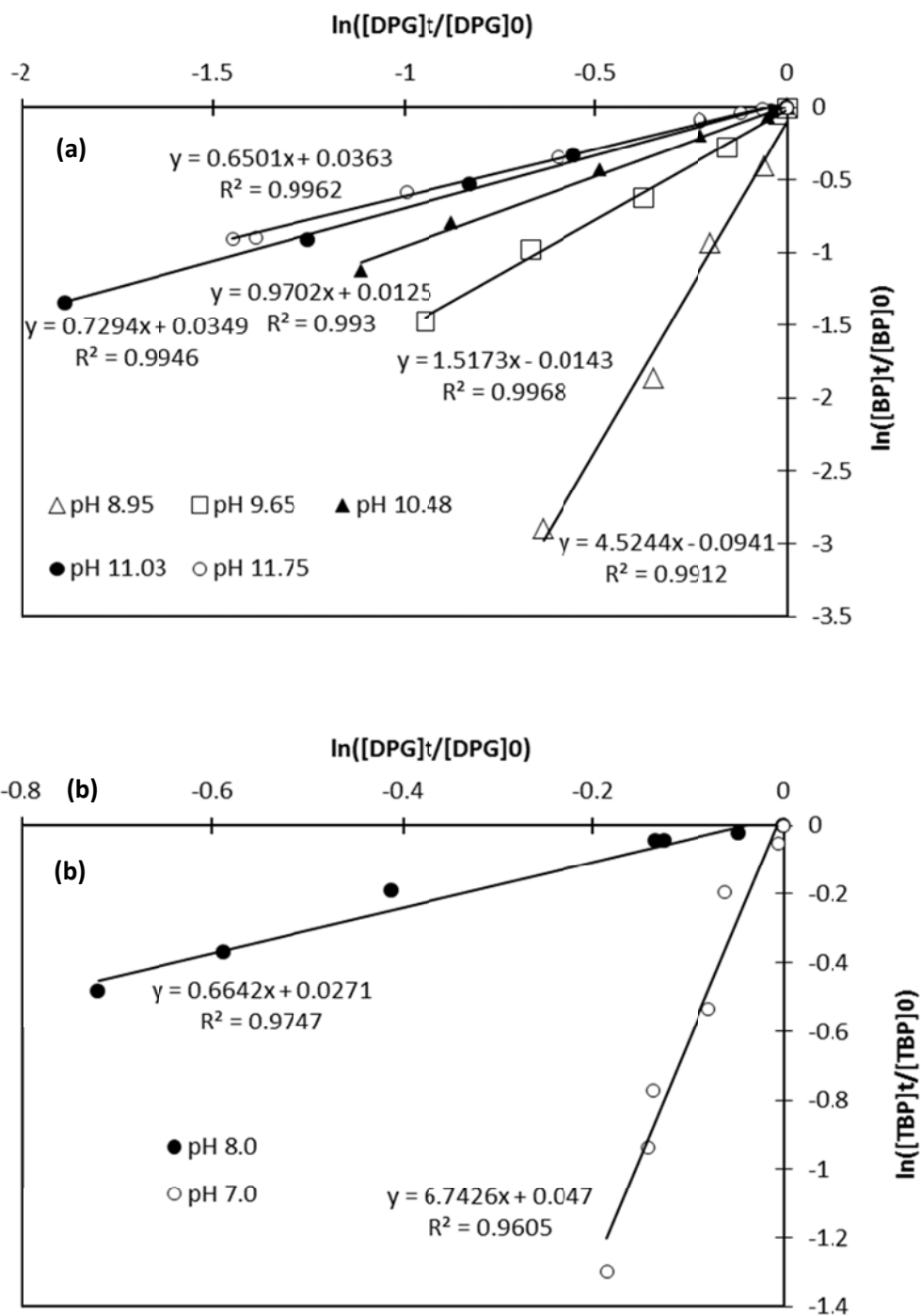


Figure S3. Determination of apparent second order rate constants for bromination of DPG by using competition kinetics method with (a) 4-bromophenol (BP) and (b) 2,4,6-tribromophenol (TBP) as reference compound ($[DPG]_0$ 5 μ M, $[BP]_0$ or $[TBP]_0$ 5 μ M, $[\text{bromine}]_0$ 0 to 10 μ M, phosphate buffer 10 mM)

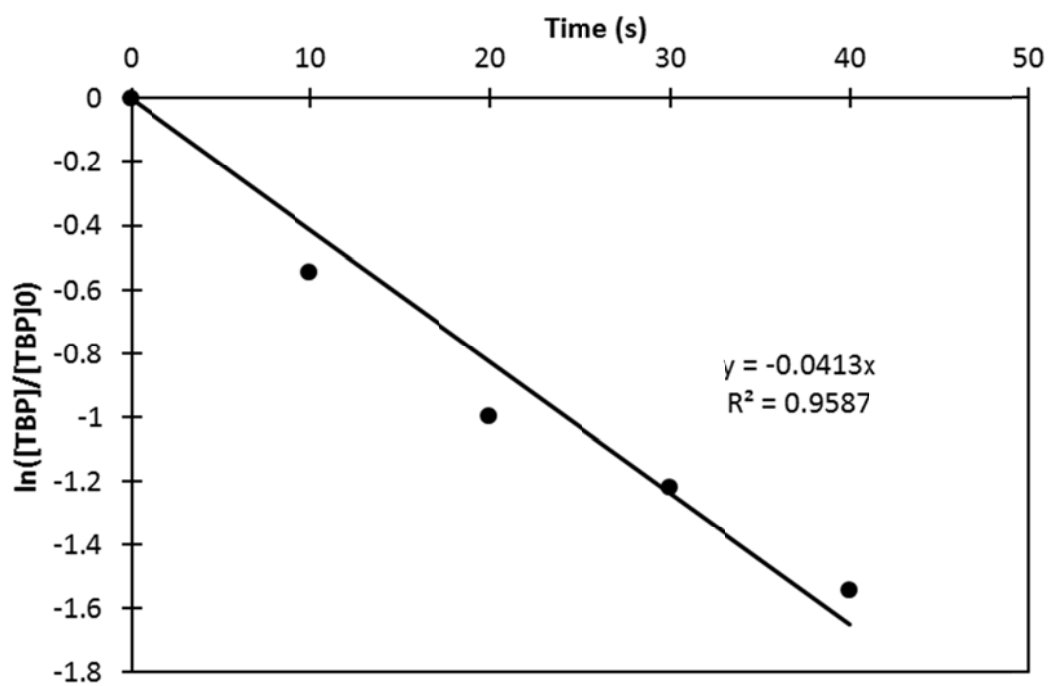


Figure S4. Determination of apparent rate constant of bromination of TBP (pH 6.94, [TBP]₀ 1 μM, [bromine]₀ 20 μM, 10 mM phosphate buffer)

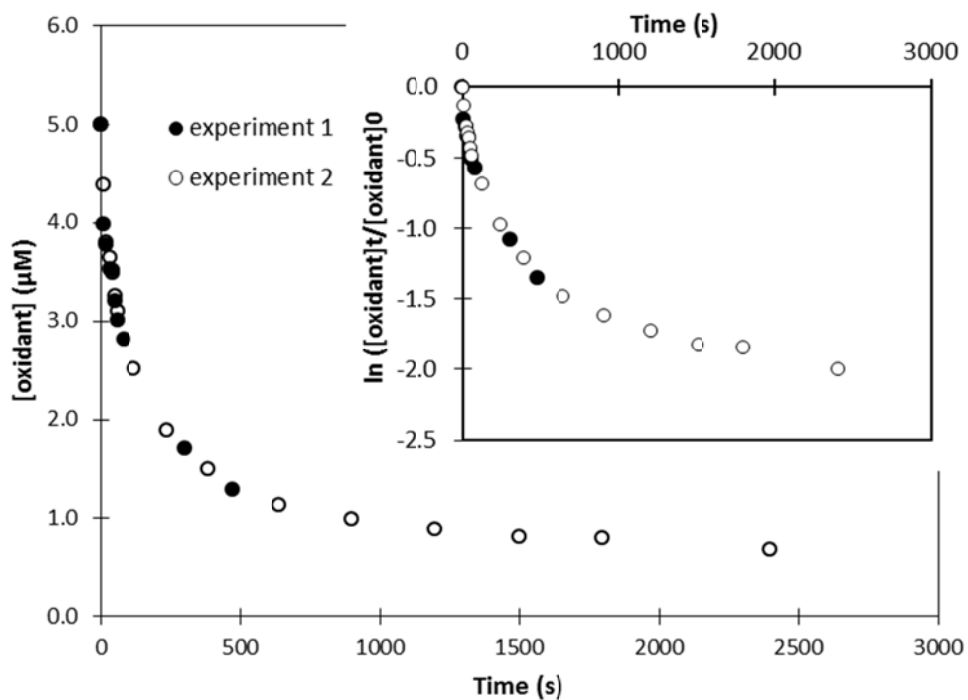


Figure S5. Decay of oxidant response during bromination of DPG (pH 6.9, $[\text{DPG}]_0$ 50 μM , $[\text{bromine}]_0$ 5 μM , phosphate buffer 10 mM)

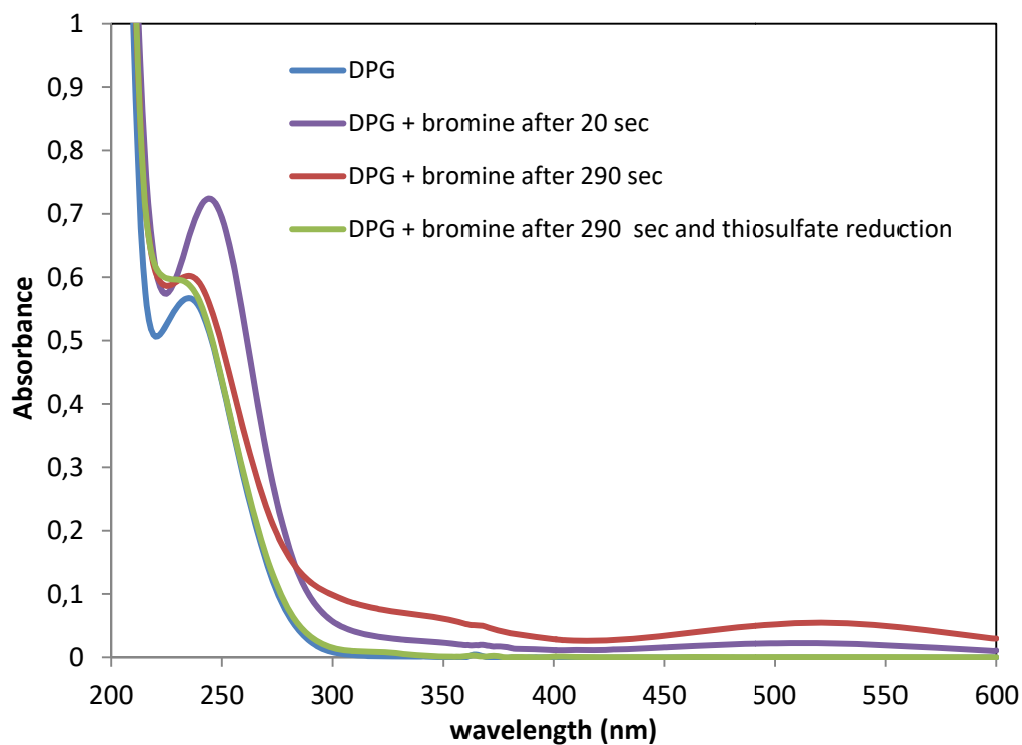


Figure S6. UV/visible spectra of DPG solution before and after bromine addition (pH 6.9, 10 mM phosphate buffer, $[\text{DPG}]_0$ 50 μM , $[\text{Br}_2]_0$ 50 μM , reduction by an excess of thiosulfate)

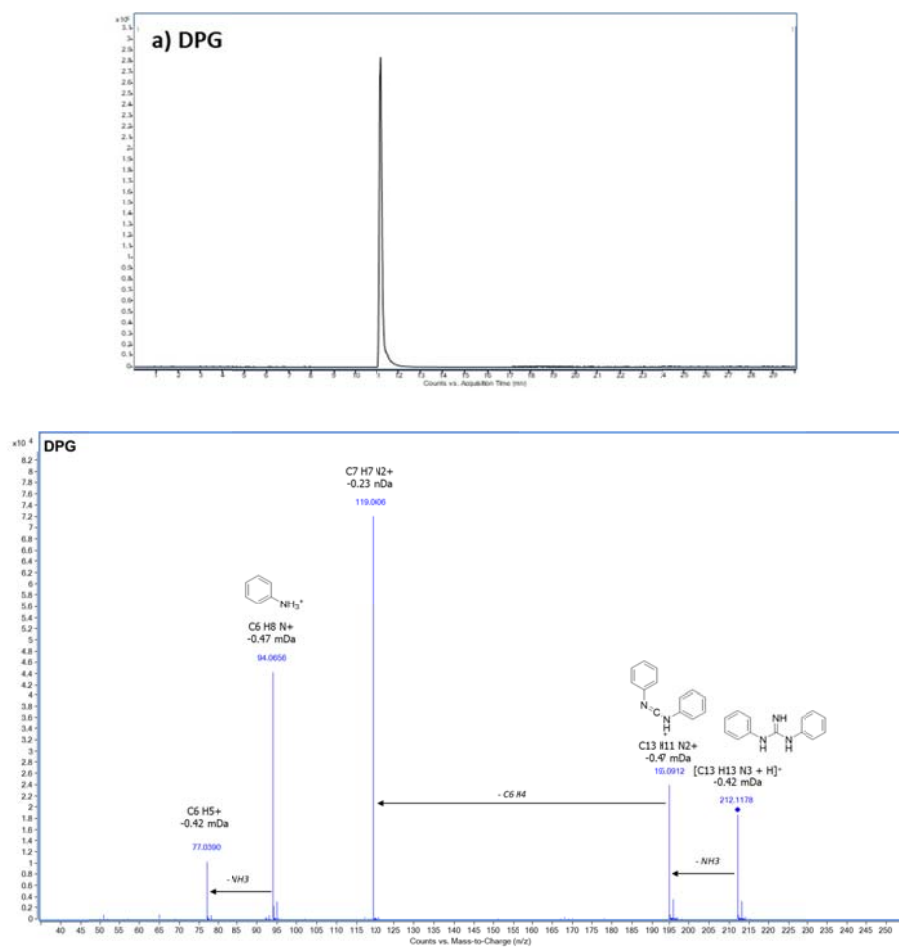


Figure S7. Chromatograms and MS/MS spectra of DPG and its TPs.

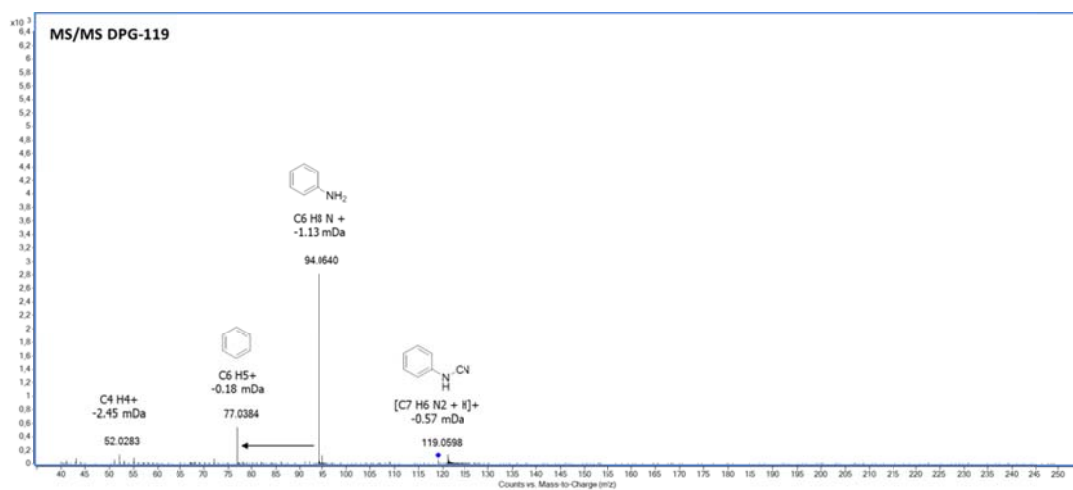
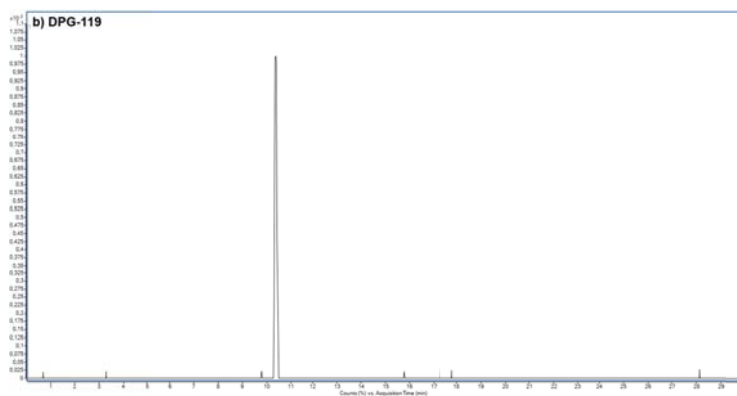


Figure S7. Chromatograms and MS/MS spectra of DPG and its TPs. *Continued.*

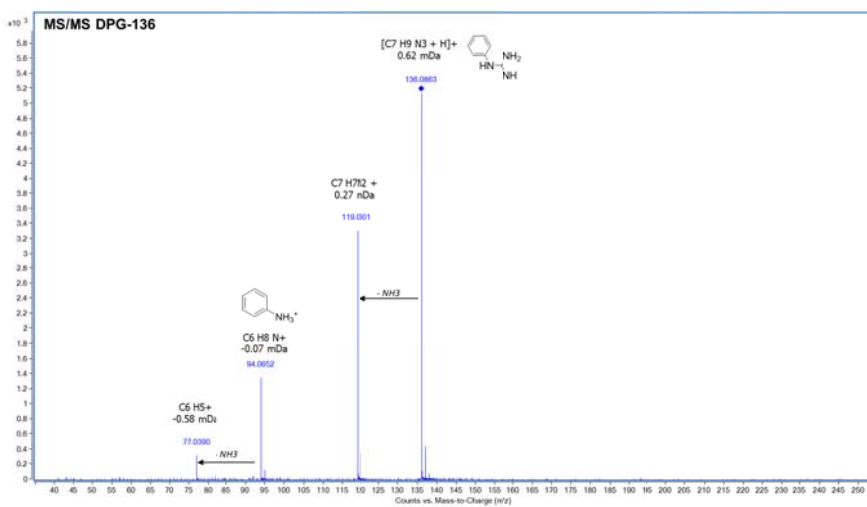
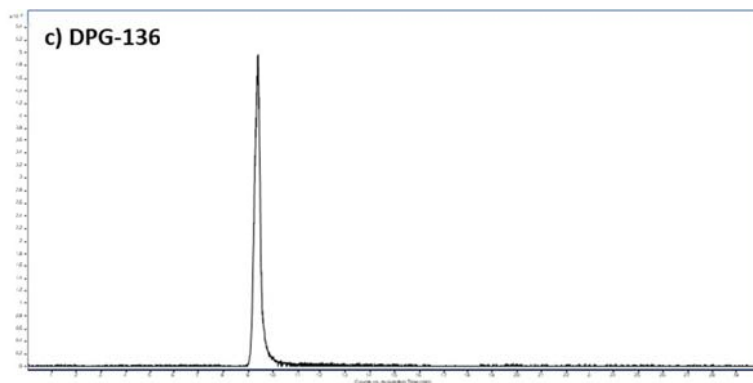


Figure S7. Chromatograms and MS/MS spectra of DPG and its TPs. *Continued.*

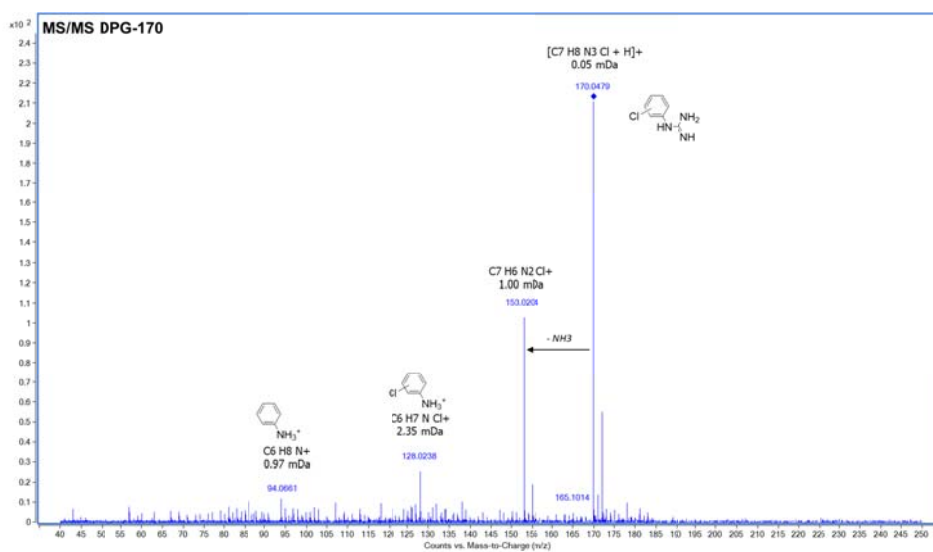
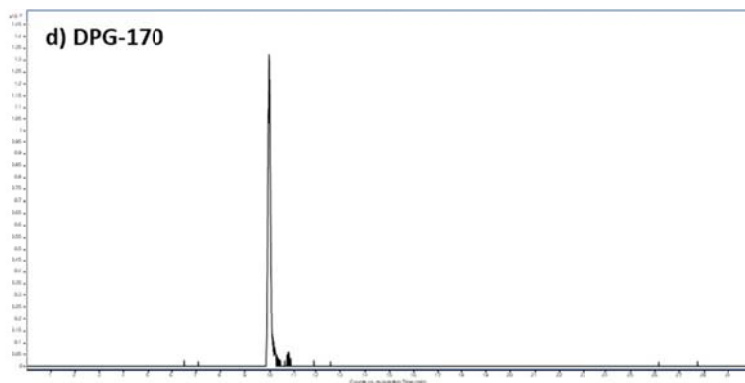


Figure S7. Chromatograms and MS/MS spectra of DPG and its TPs. *Continued.*

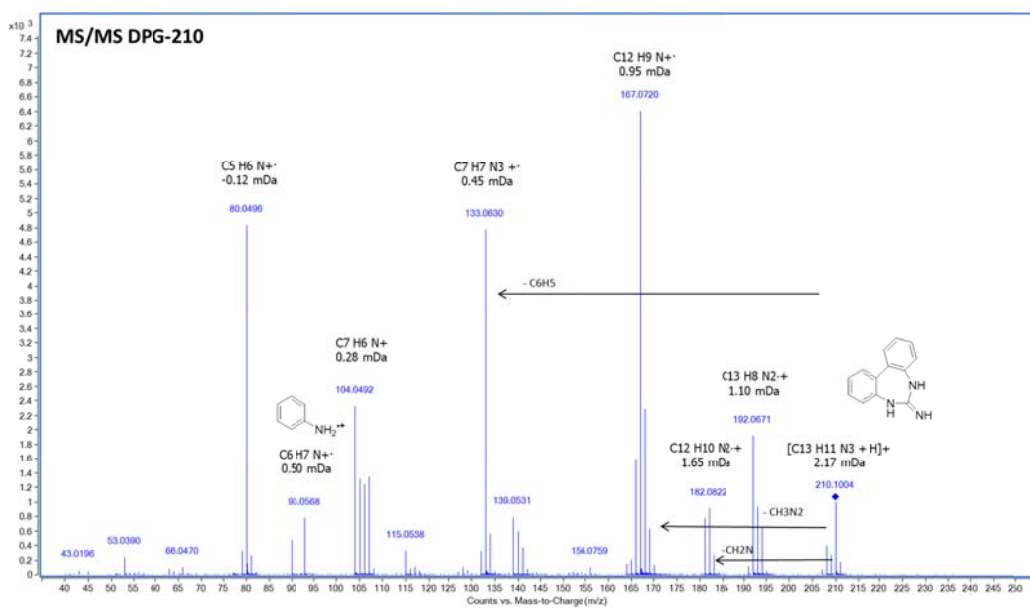
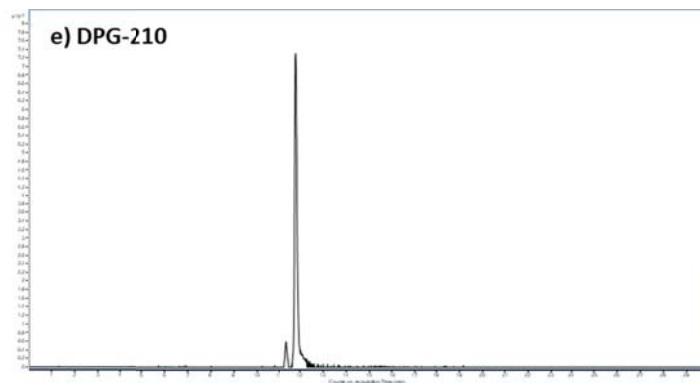


Figure S7. Chromatograms and MS/MS spectra of DPG and its TPs. *Continued.*

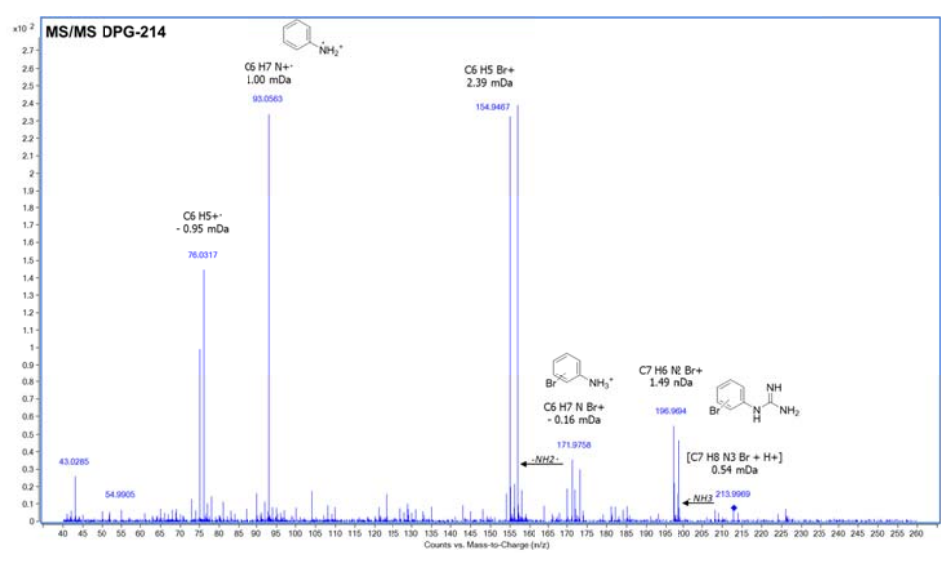
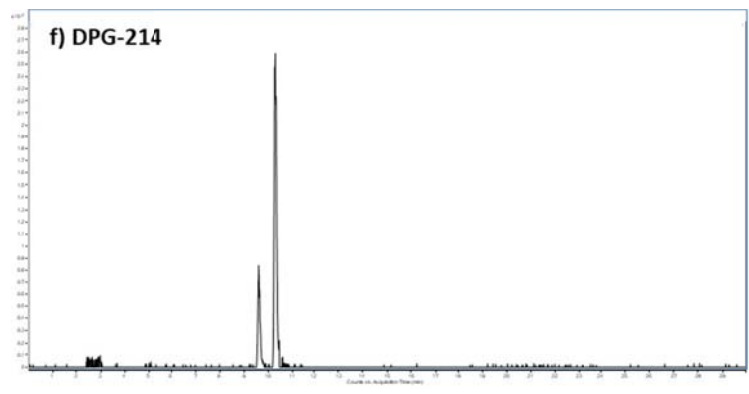


Figure S7. Chromatograms and MS/MS spectra of DPG and its TPs. *Continued.*

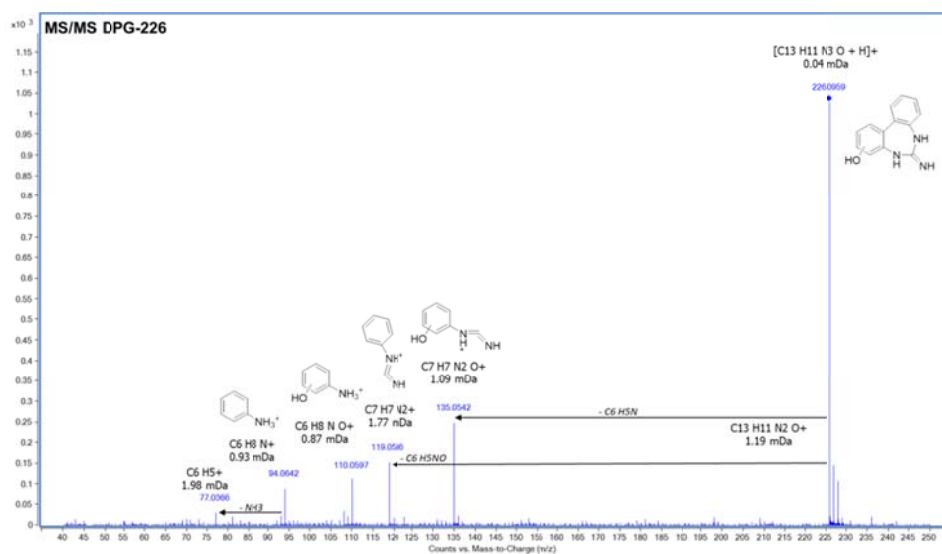
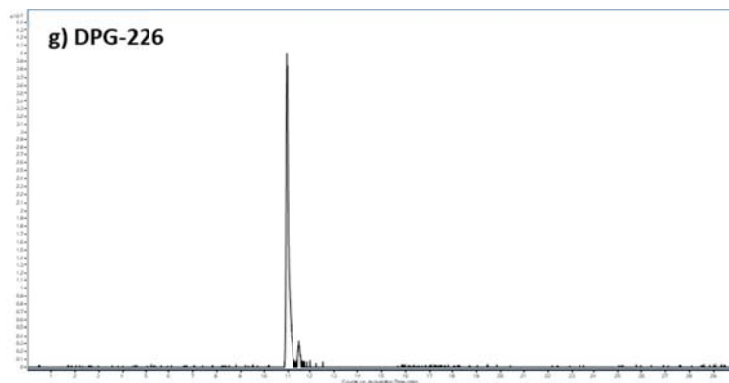


Figure S7. Chromatograms and MS/MS spectra of DPG and its TPs. *Continued.*

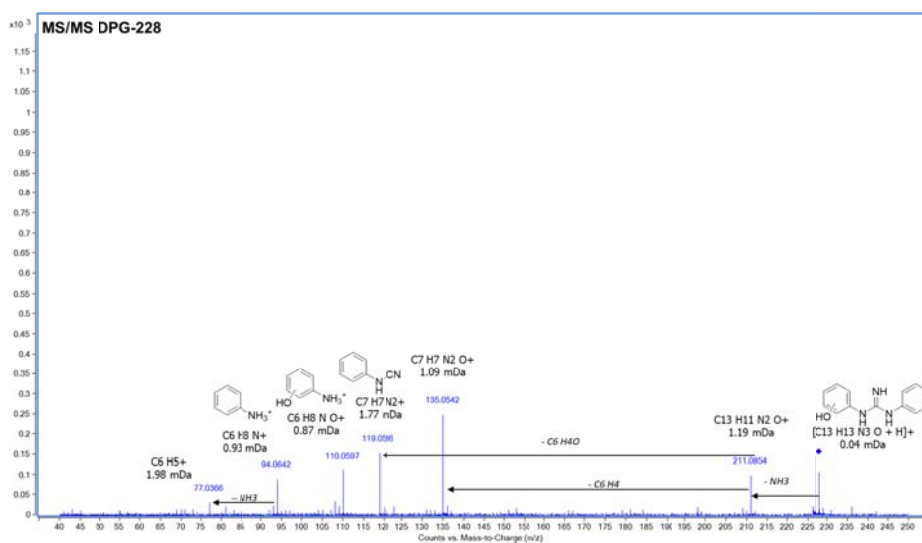
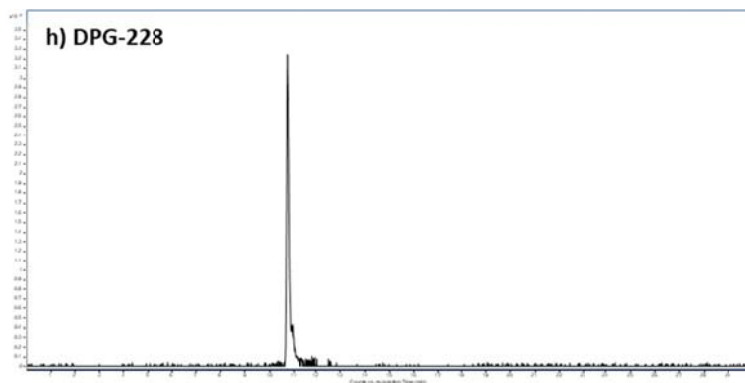


Figure S7. Chromatograms and MS/MS spectra of DPG and its TPs. *Continued.*

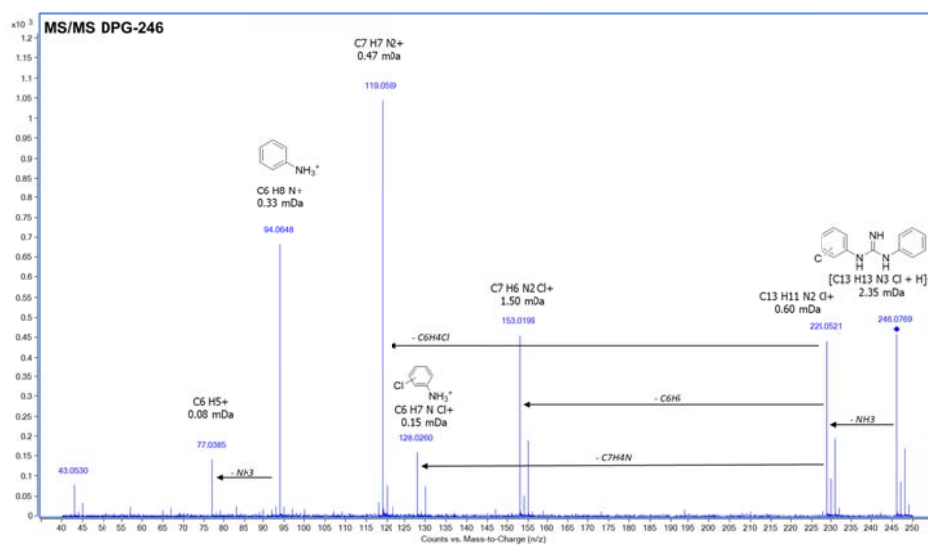
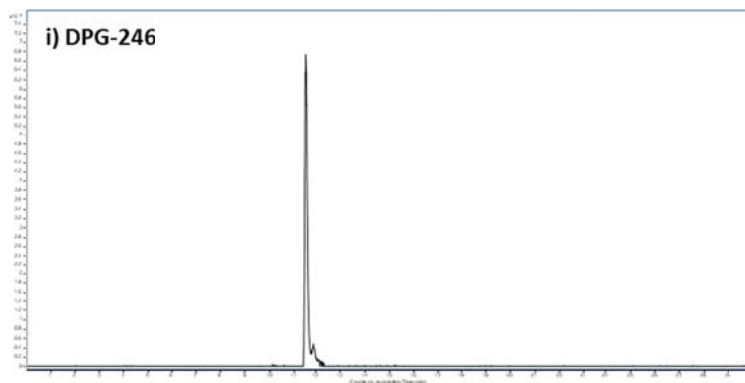


Figure S7. Chromatograms and MS/MS spectra of DPG and its TPs. *Continued.*

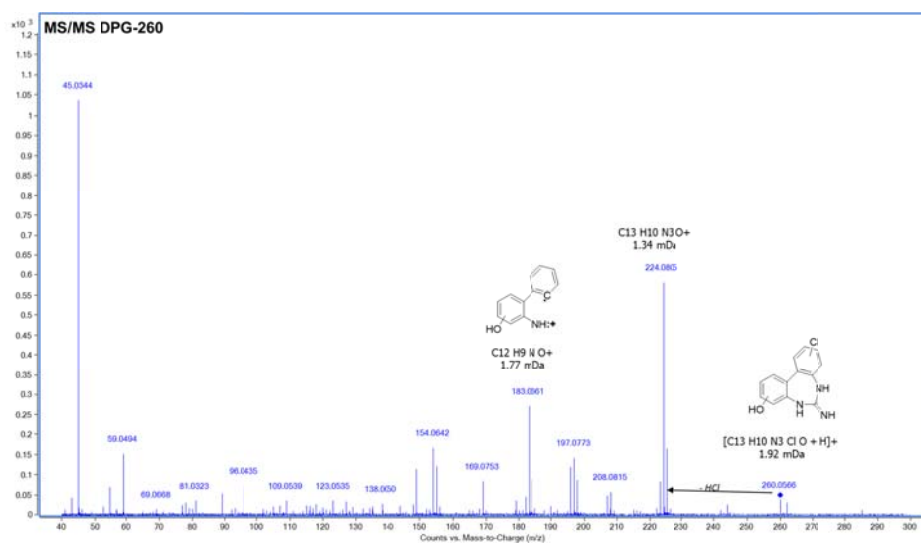
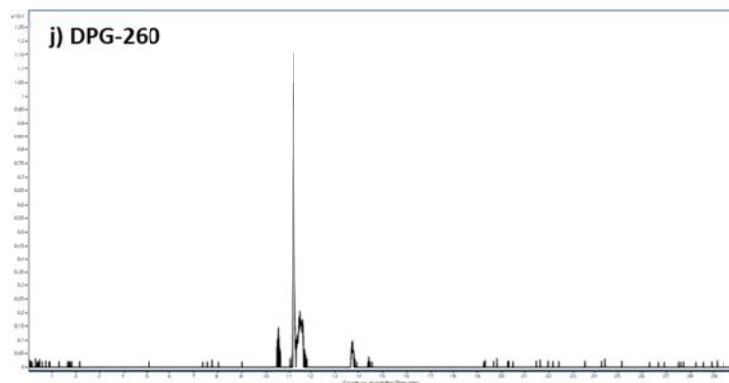


Figure S7. Chromatograms and MS/MS spectra of DPG and its TPs. *Continued.*

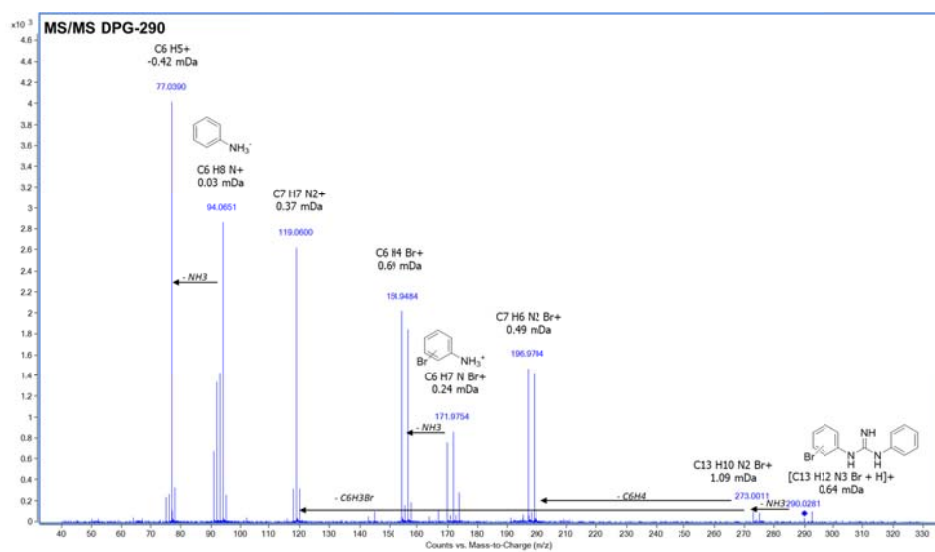
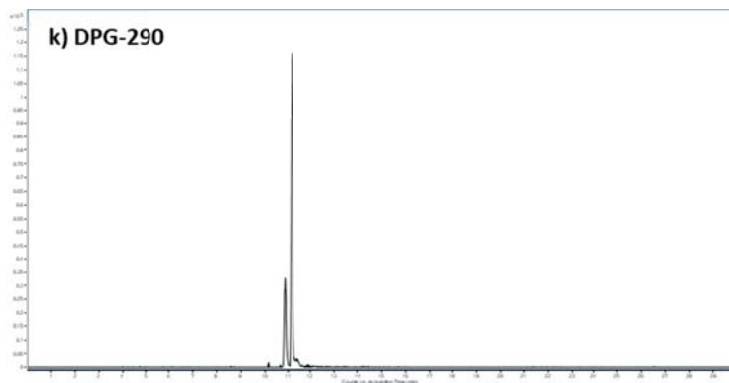


Figure S7. Chromatograms and MS/MS spectra of DPG and its TPs. *Continued.*

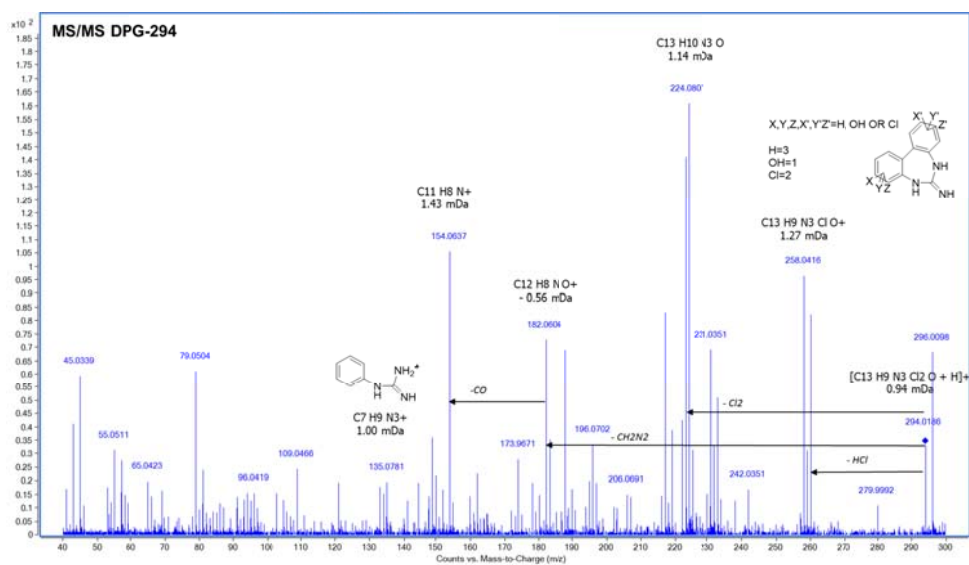
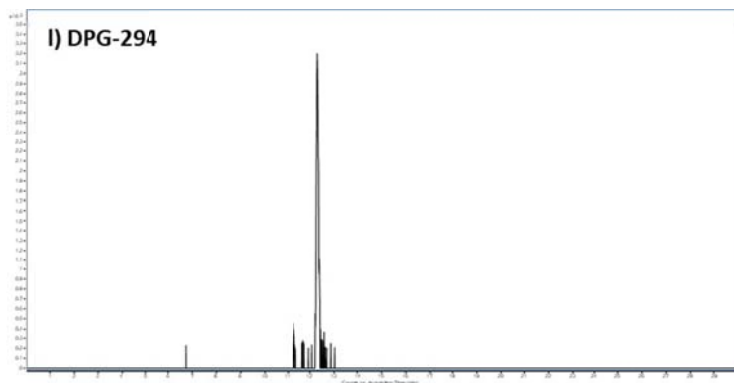


Figure S7. Chromatograms and MS/MS spectra of DPG and its TPs. *Continued.*

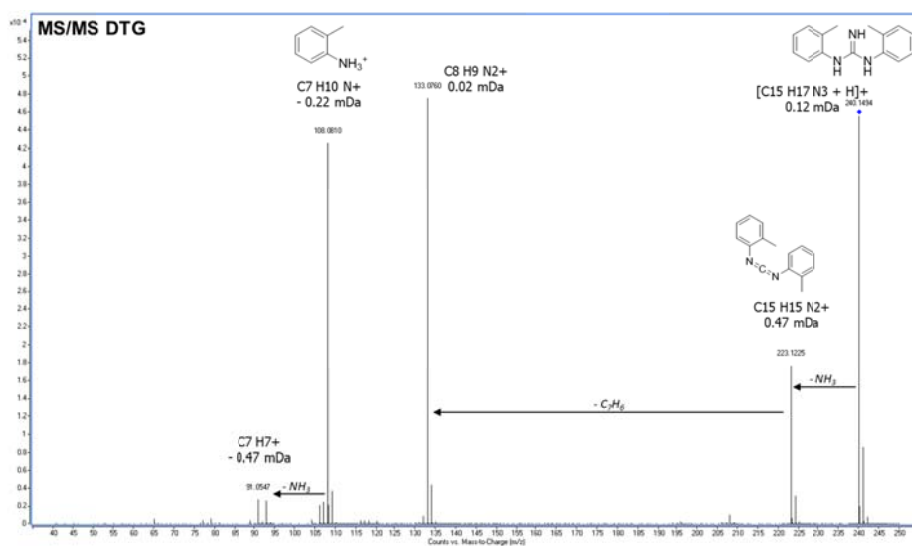
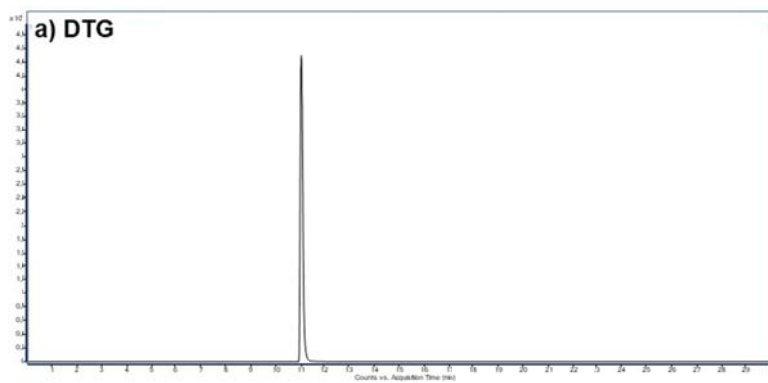


Figure S8. Chromatograms and MS/MS spectra of DTG and its TPs.

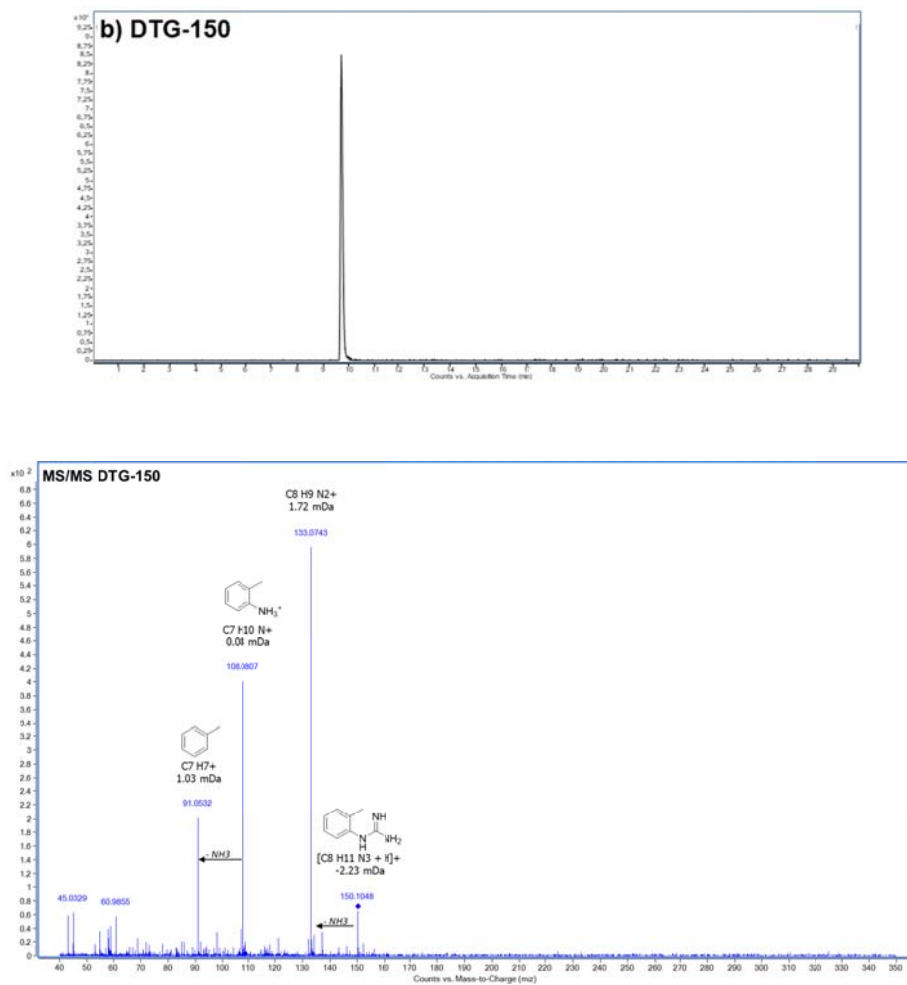


Figure S8. Chromatograms and MS/MS spectra of DTG and its TPs. *Continued.*

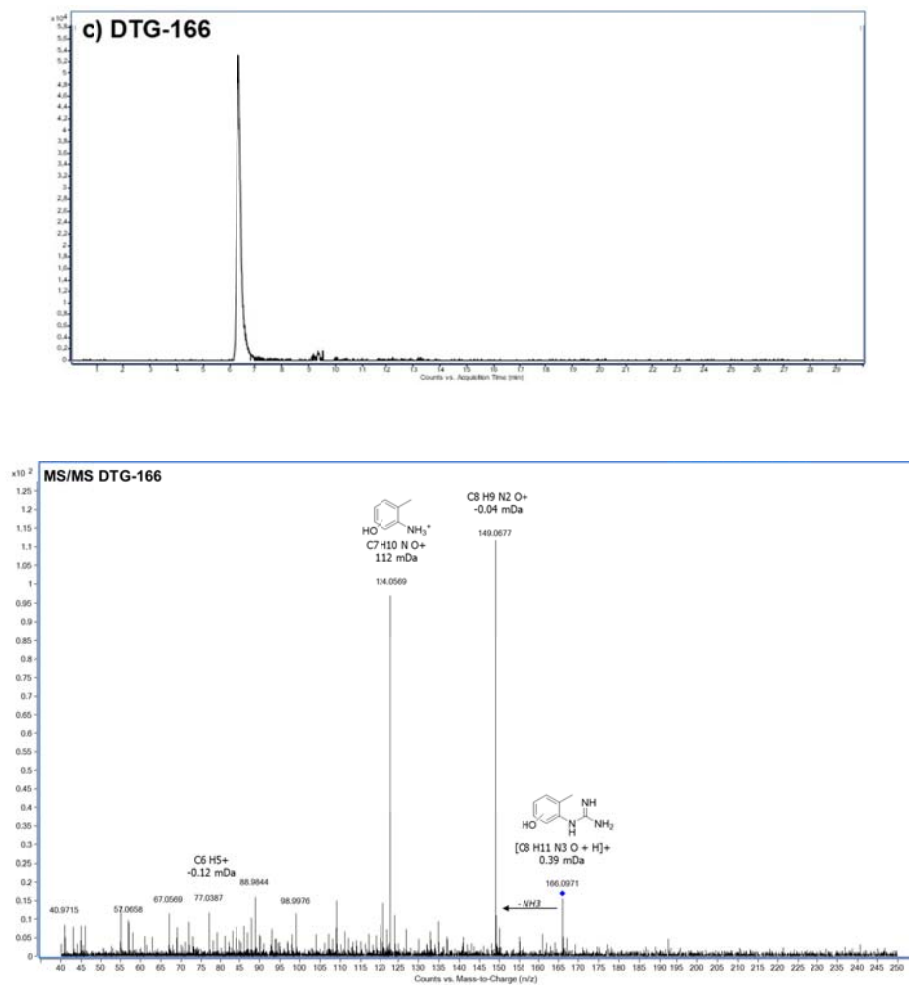


Figure S8. Chromatograms and MS/MS spectra of DTG and its TPs. *Continued.*

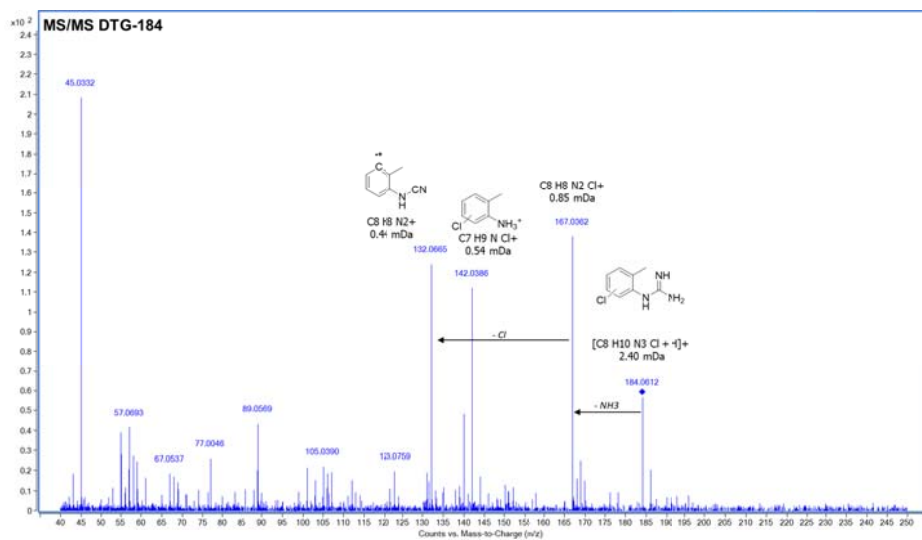
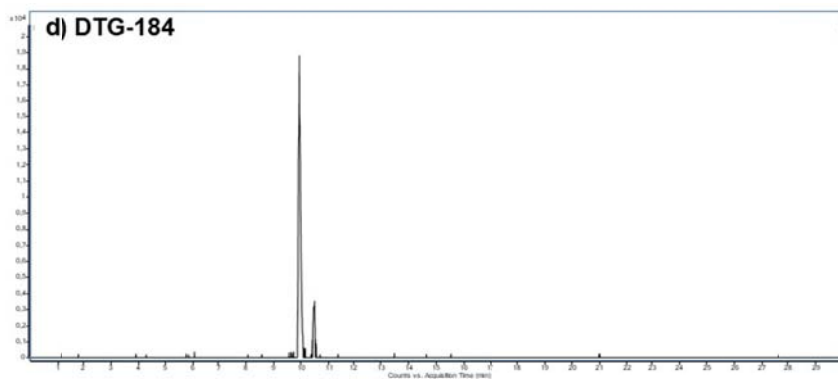


Figure S8. Chromatograms and MS/MS spectra of DTG and its TPs. *Continued.*

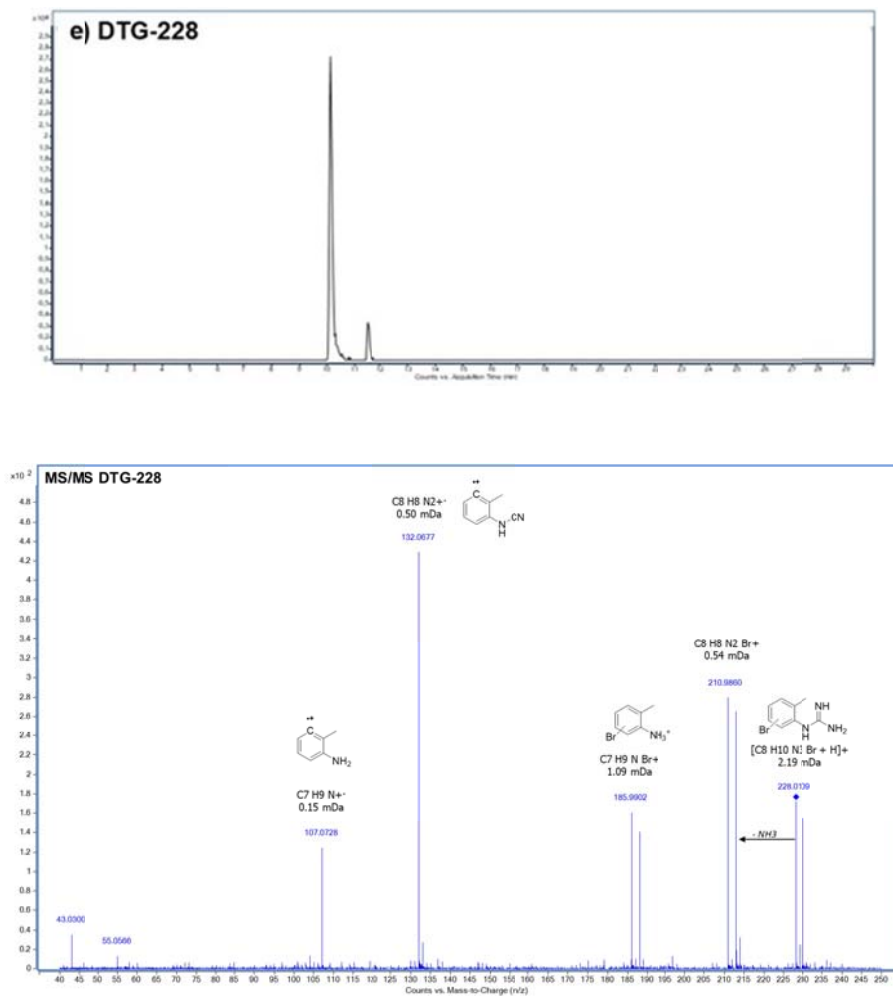


Figure S8. Chromatograms and MS/MS spectra of DTG and its TPs. *Continued.*

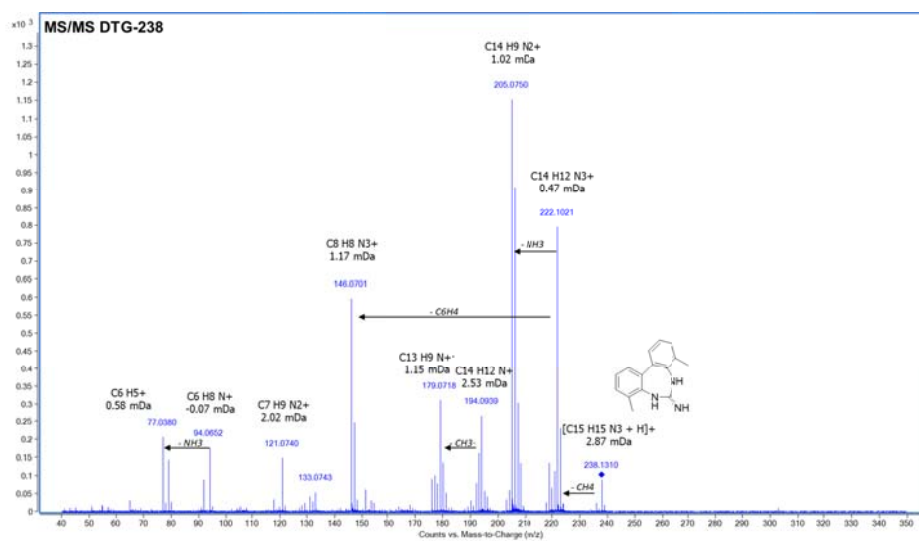
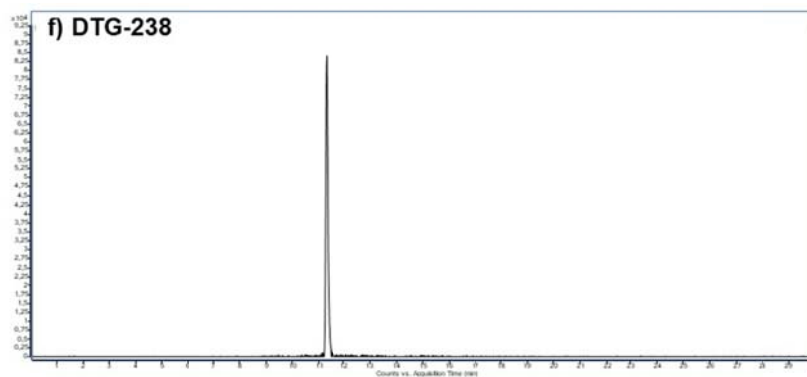


Figure S8. Chromatograms and MS/MS spectra of DTG and its TPs. *Continued.*

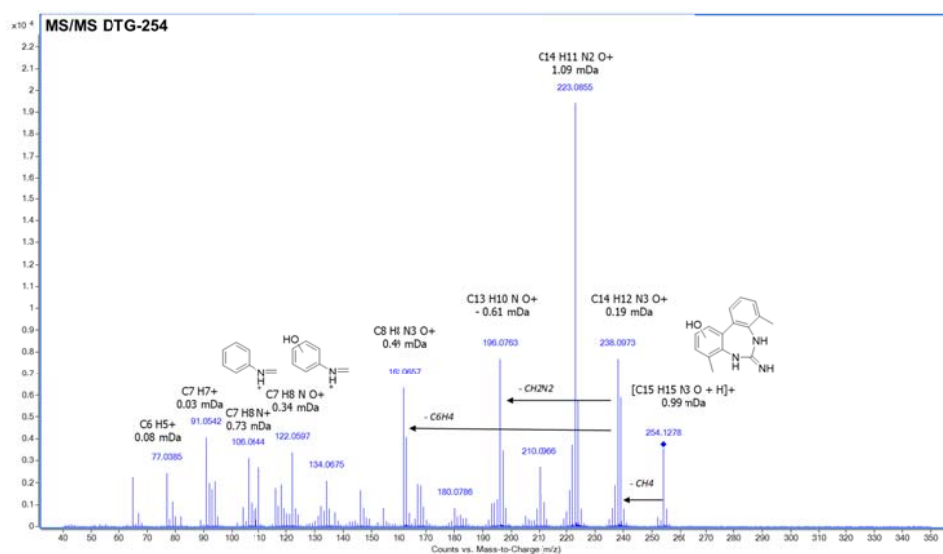
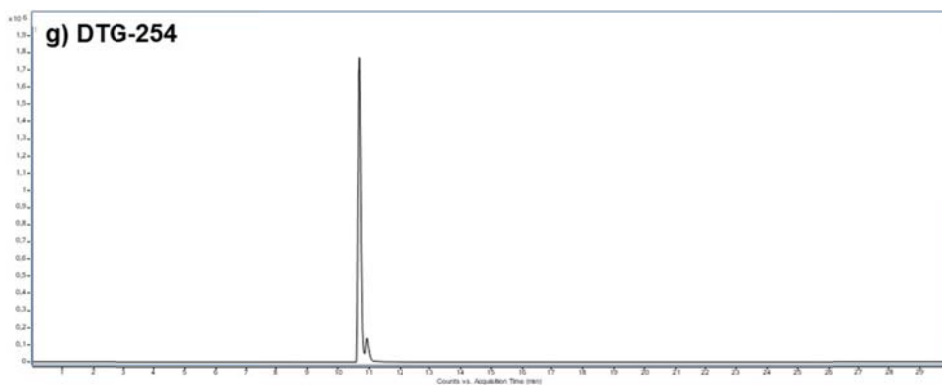


Figure S8. Chromatograms and MS/MS spectra of DTG and its TPs. *Continued.*

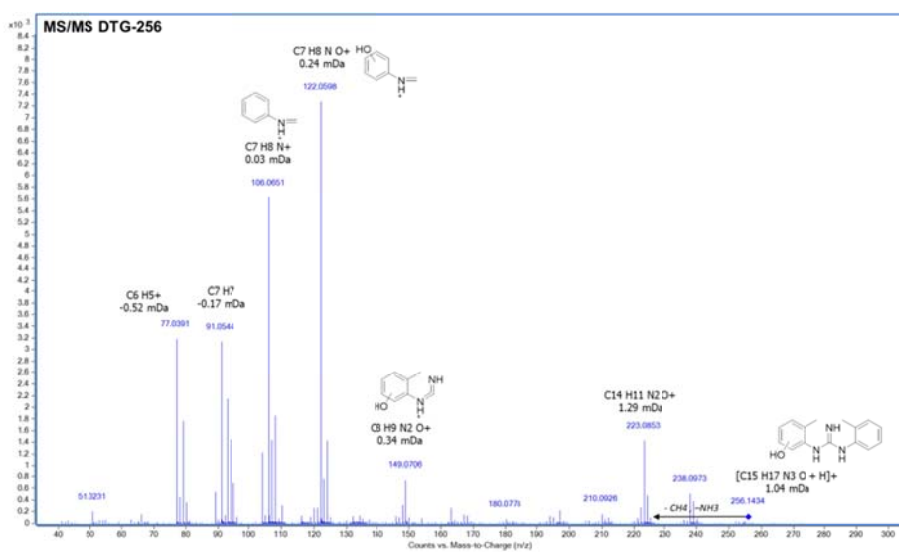
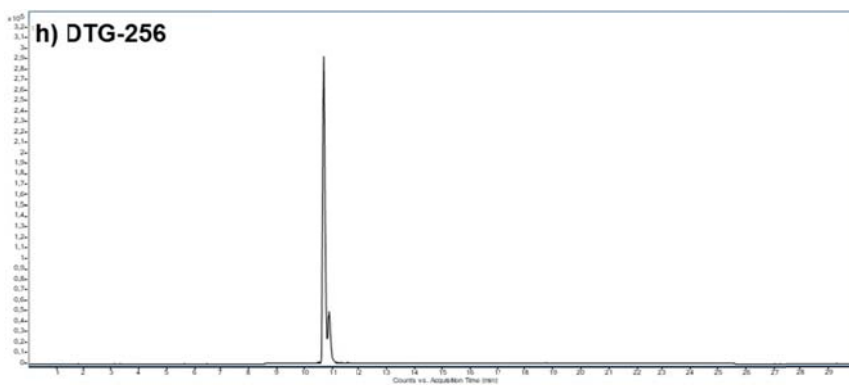


Figure S8. Chromatograms and MS/MS spectra of DTG and its TPs. *Continued.*

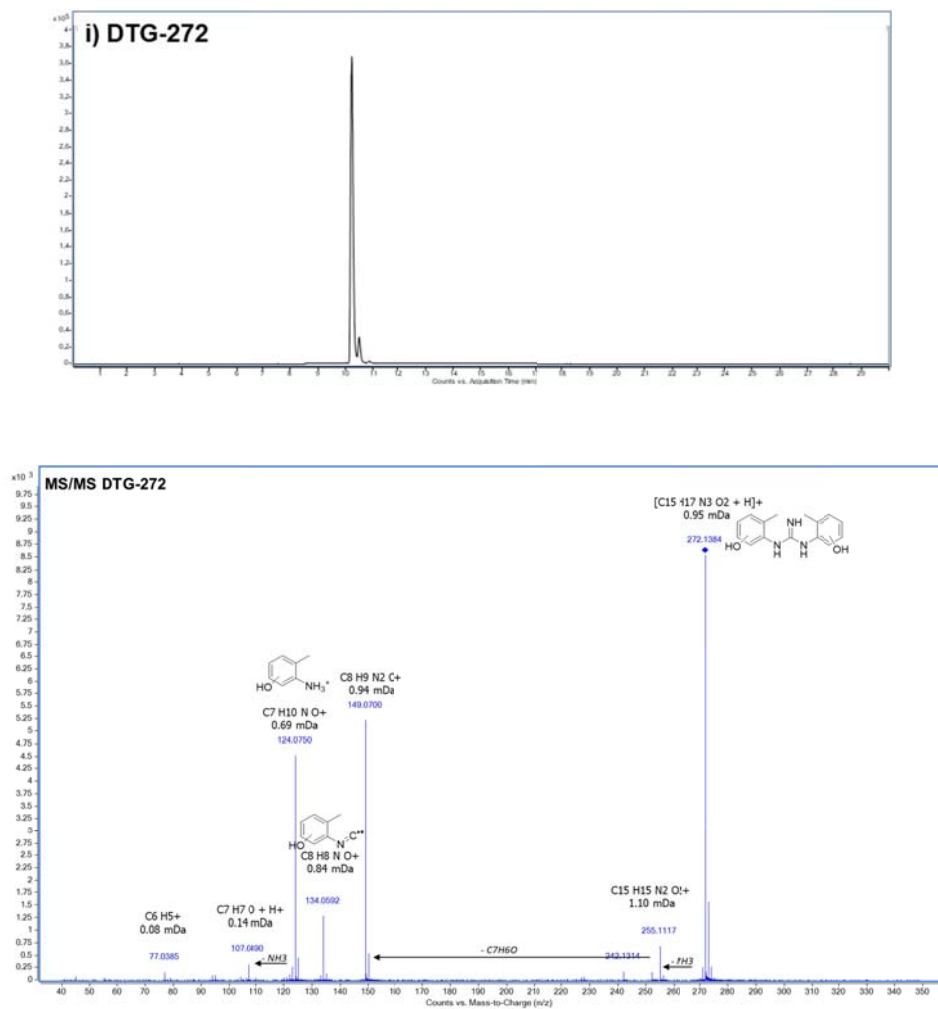


Figure S8. Chromatograms and MS/MS spectra of DTG and its TPs. *Continued.*

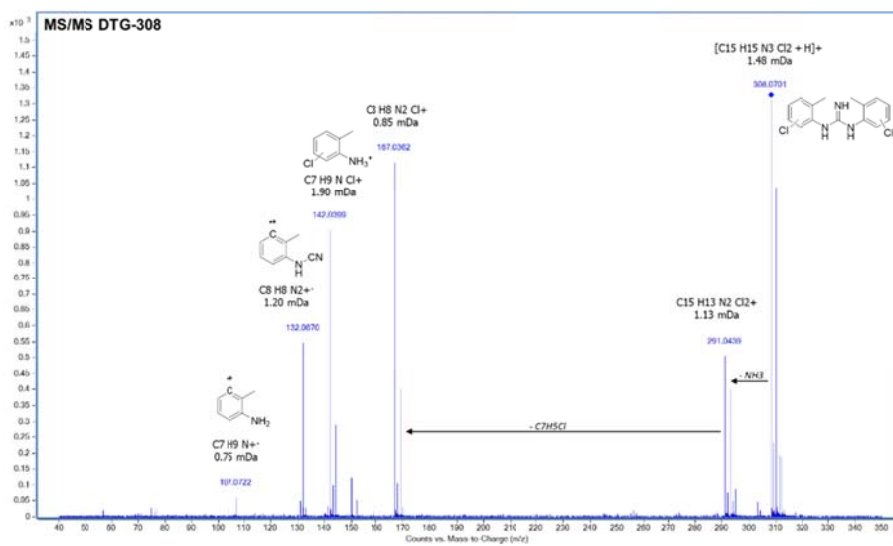
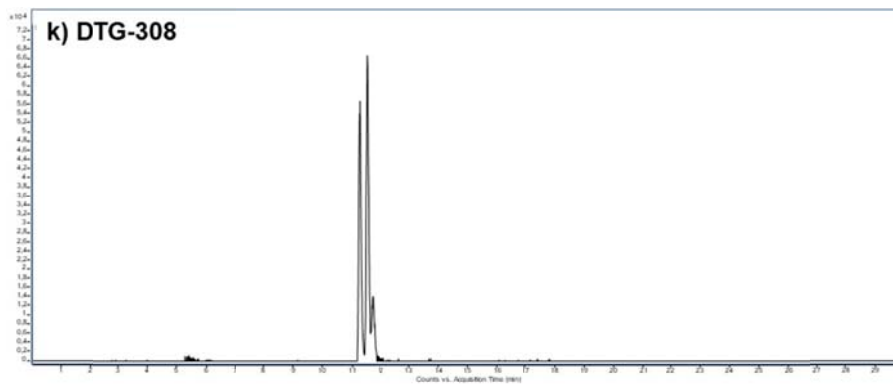


Figure S8. Chromatograms and MS/MS spectra of DTG and its TPs. *Continued.*

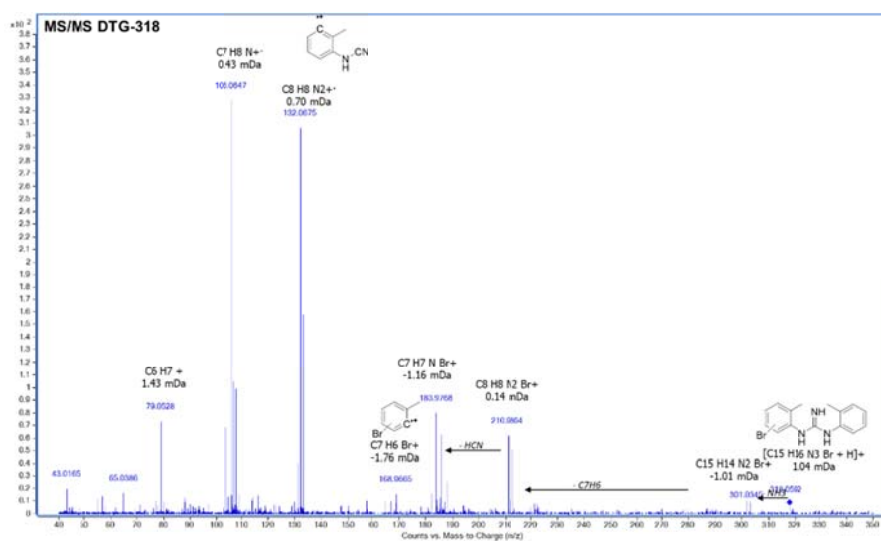
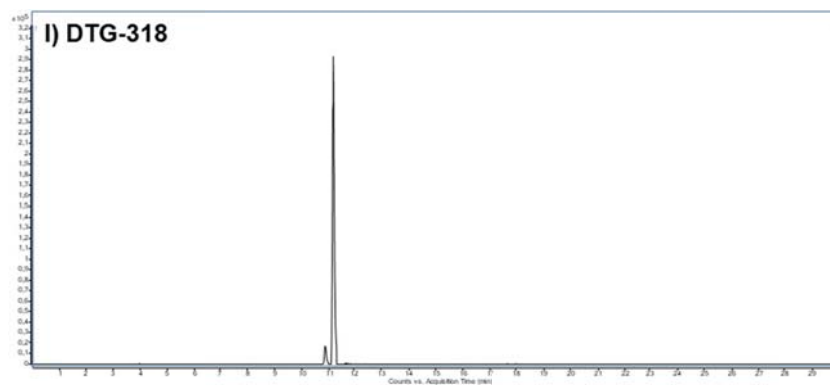


Figure S8. Chromatograms and MS/MS spectra of DTG and its TPs. *Continued.*

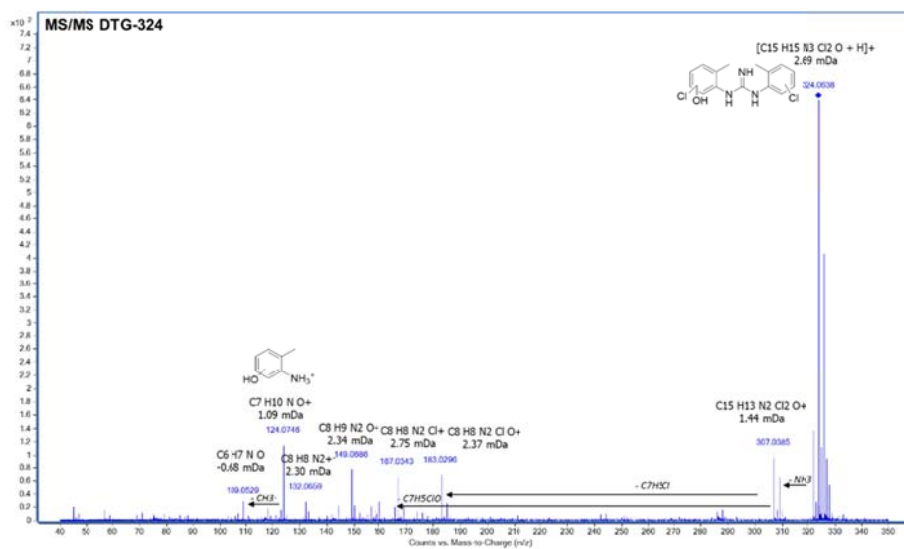
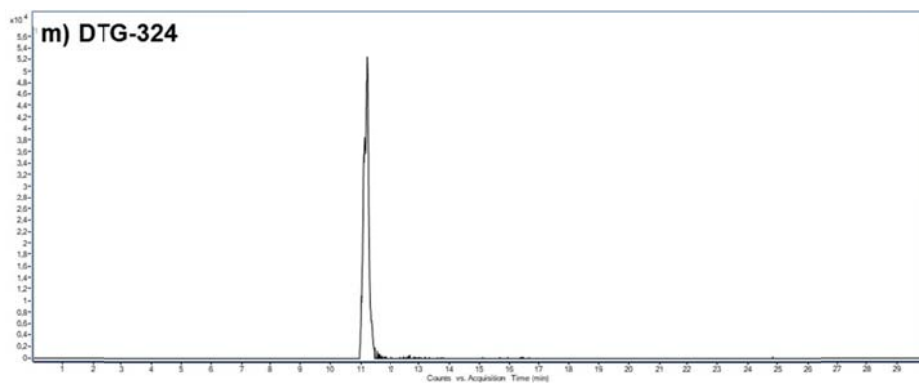


Figure S8. Chromatograms and MS/MS spectra of DTG and its TPs. *Continued.*

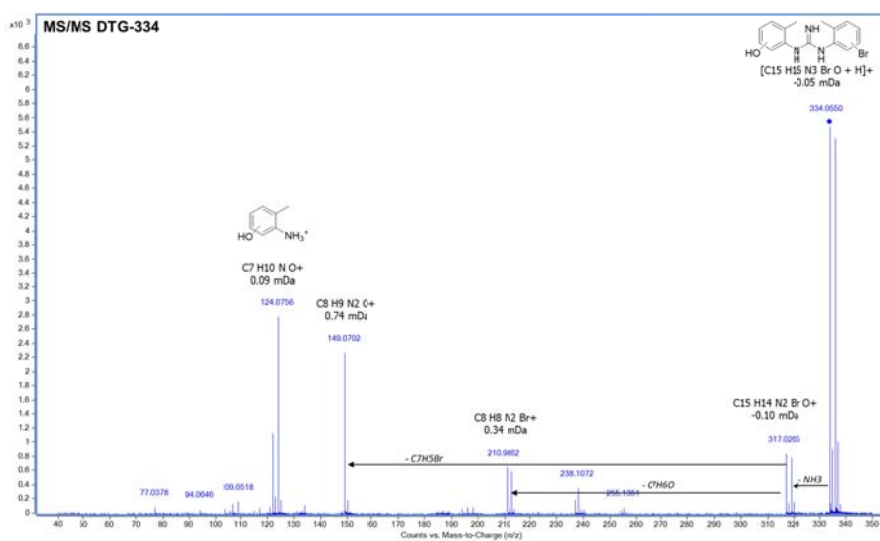
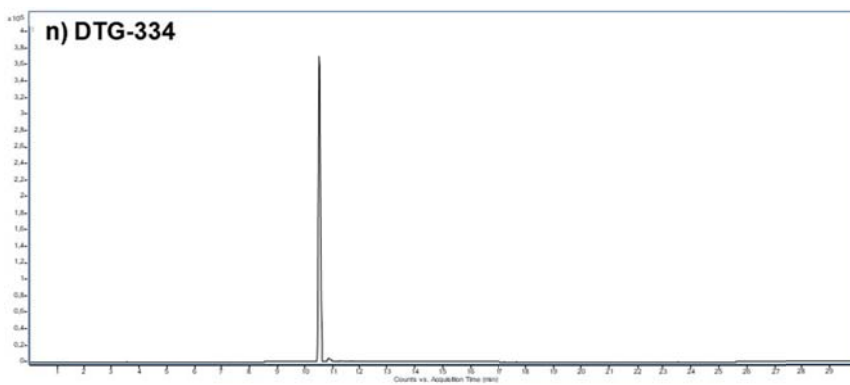


Figure S8. Chromatograms and MS/MS spectra of DTG and its TPs. *Continued.*

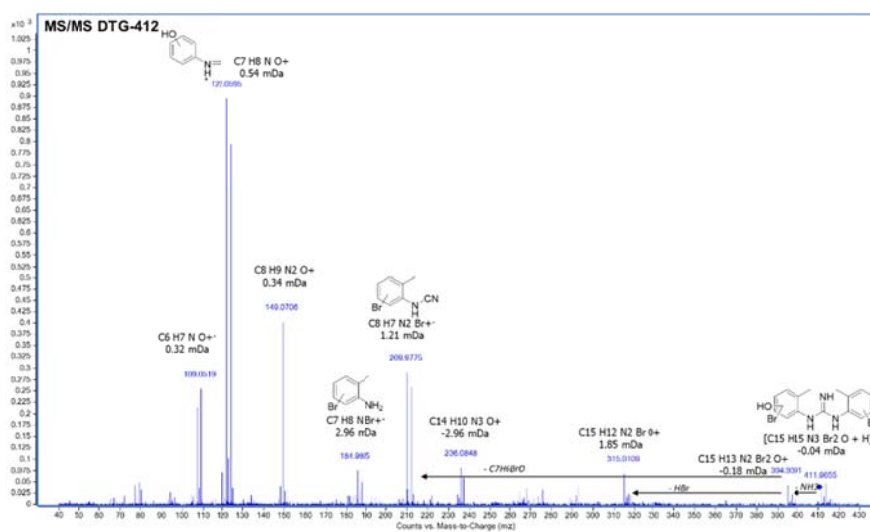
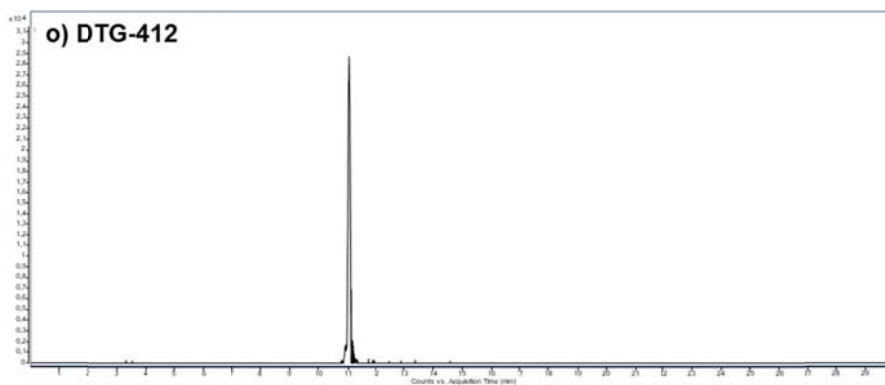


Figure S8. Chromatograms and MS/MS spectra of DTG and its TPs. *Continued.*

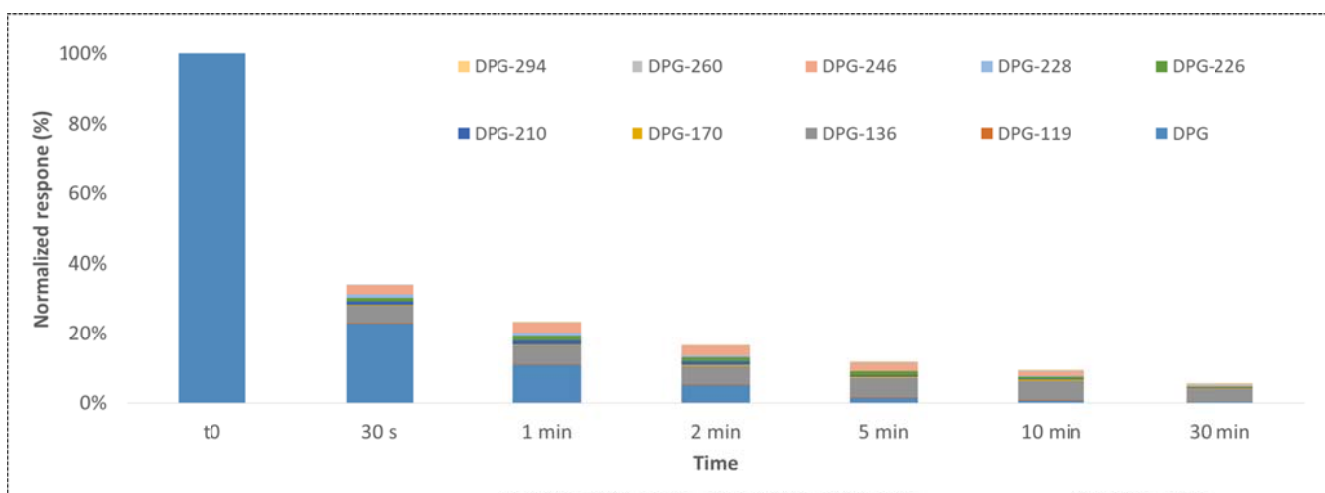
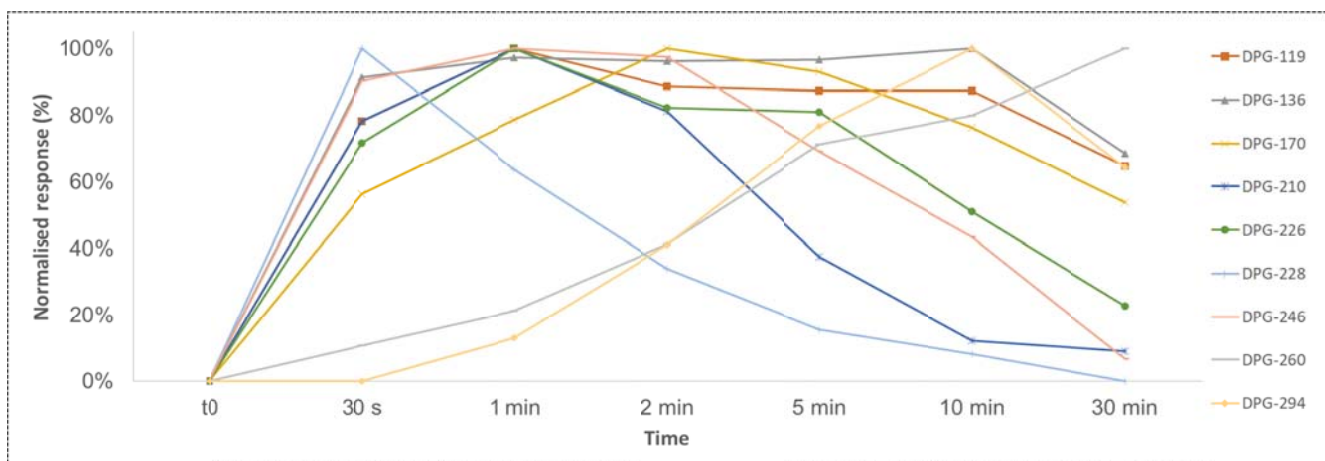


Figure S9. Plot summarizing the formation of TPs from DPG ($10 \mu\text{M DPG} + 100 \mu\text{M Cl}_2$) at different reaction times: (a) results normalized to the time when the TP reached its maximum; (b) results normalized by assuming that the response of the TPs was equal to DPG, except for DPG-136, DPG-119 and DPG-170 (where DPG-136 was used instead)

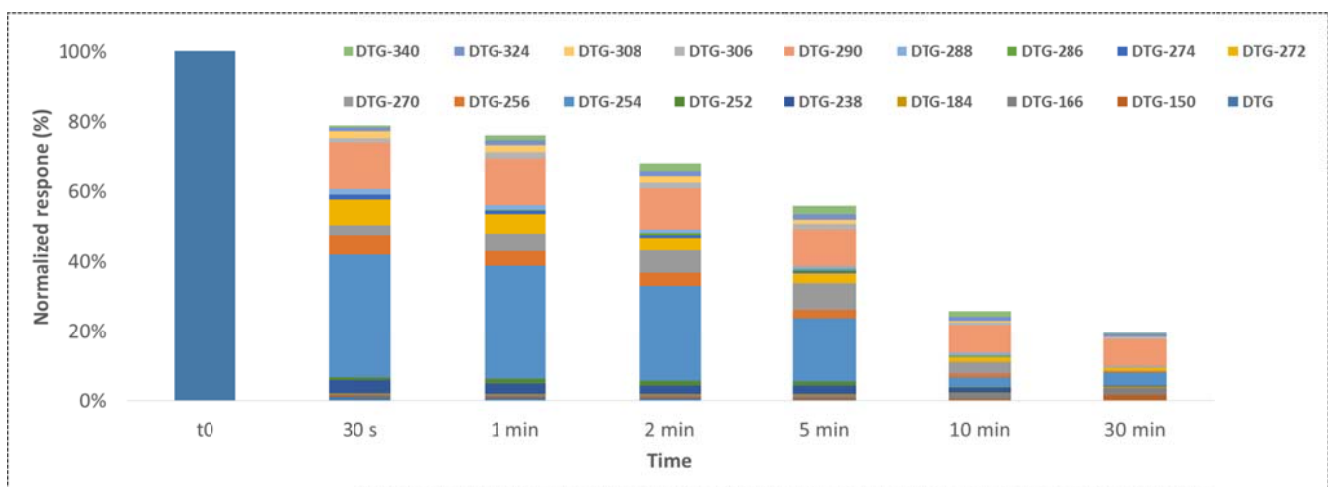
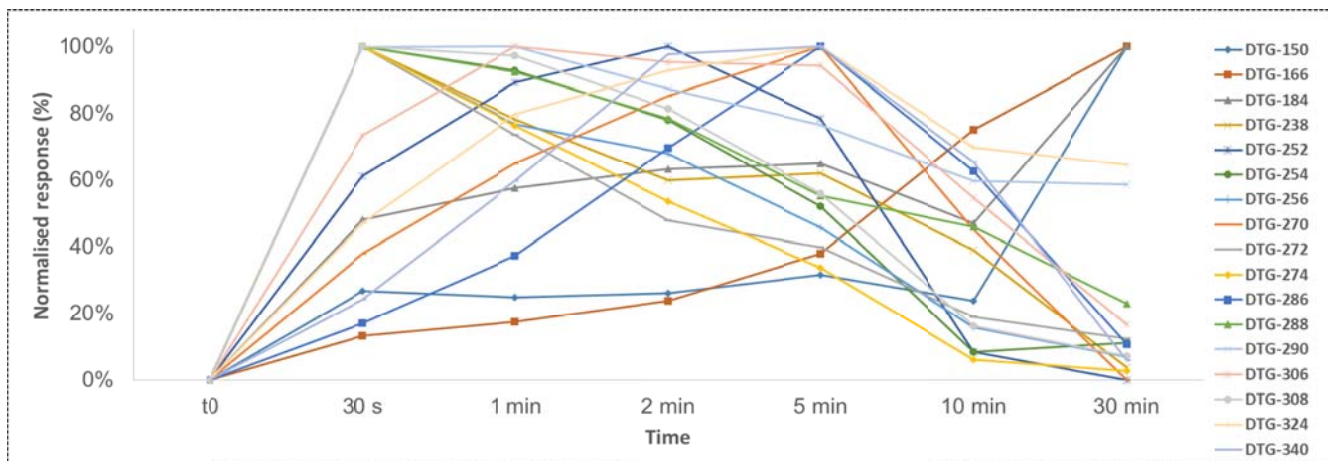


Figure S10. Plot summarizing the formation of TPs from DTG (10 μ M DTG + 100 μ M Cl₂) at different reaction times: (a) results normalized to the time when the TP reached its maximum; (b) results normalized by assuming that the response of the TPs was equal to DTG, except for DTG-150, DTG-166, DTG-184 and DTG-228 (where DPG-136 was used instead).

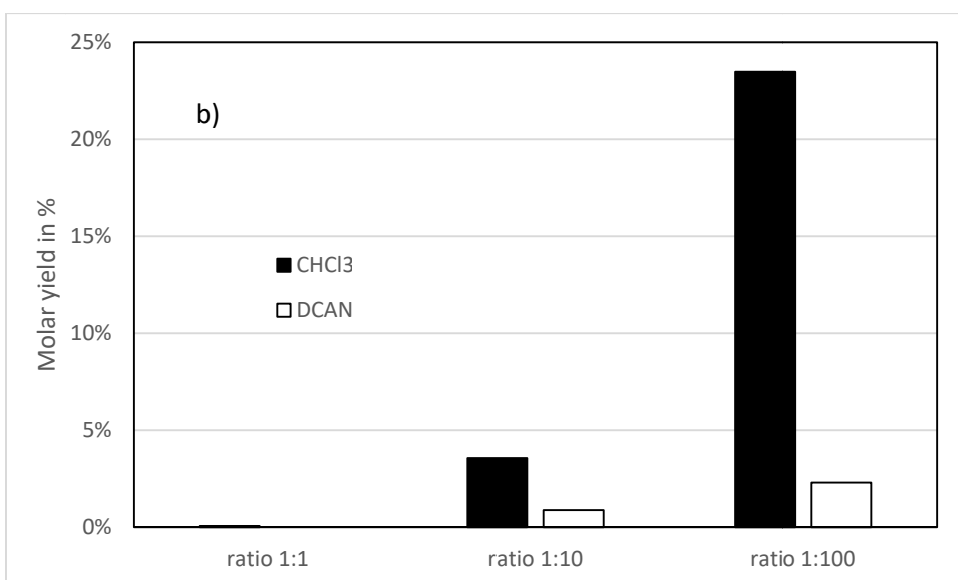
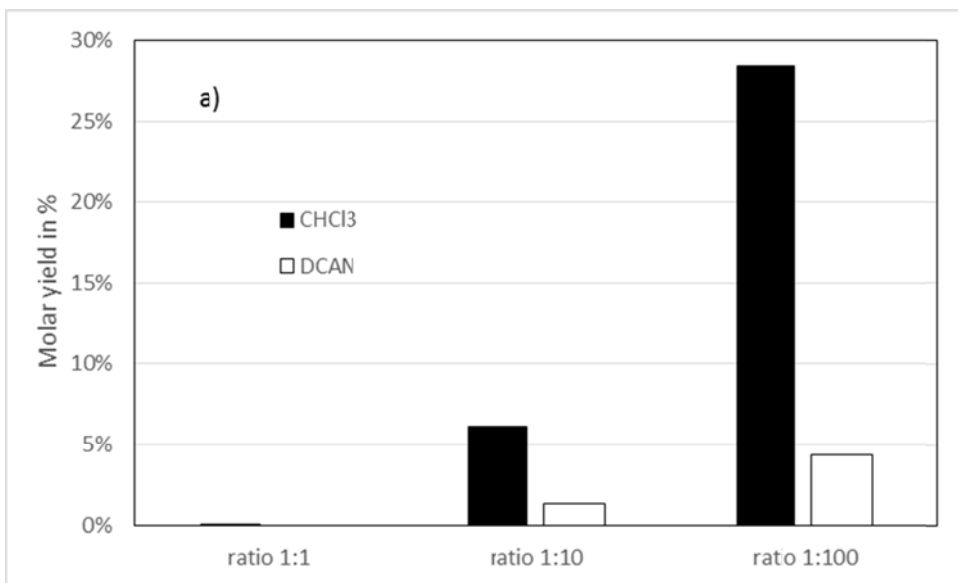


Figure S11. Molar yield of chloroform and dichloroacetonitrile (DCAN) obtained at different molar DPG/DTG:chlorine ratios: (a) DPG, (b) DTG. (pH 7.0, [DPG]₀ or [DTG]₀= 10 μ M, reaction time 48 hours).

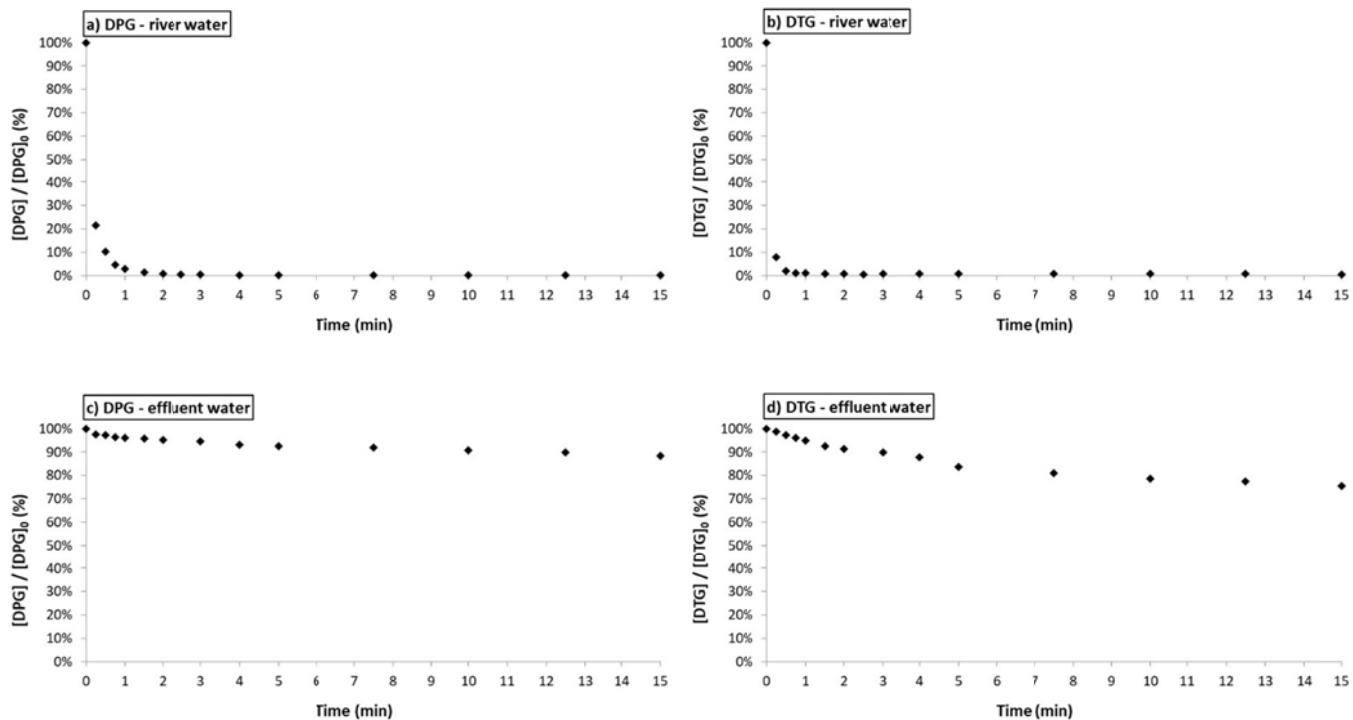


Figure S12. Dissipation plots during the chlorination of real water samples ($1 \mu\text{M}$ DPG/DTG + $10 \mu\text{M}$ Cl_2): (a) DPG in river water, (b) DTG in river water, (c) DPG in effluent, (d) DTG in effluent.

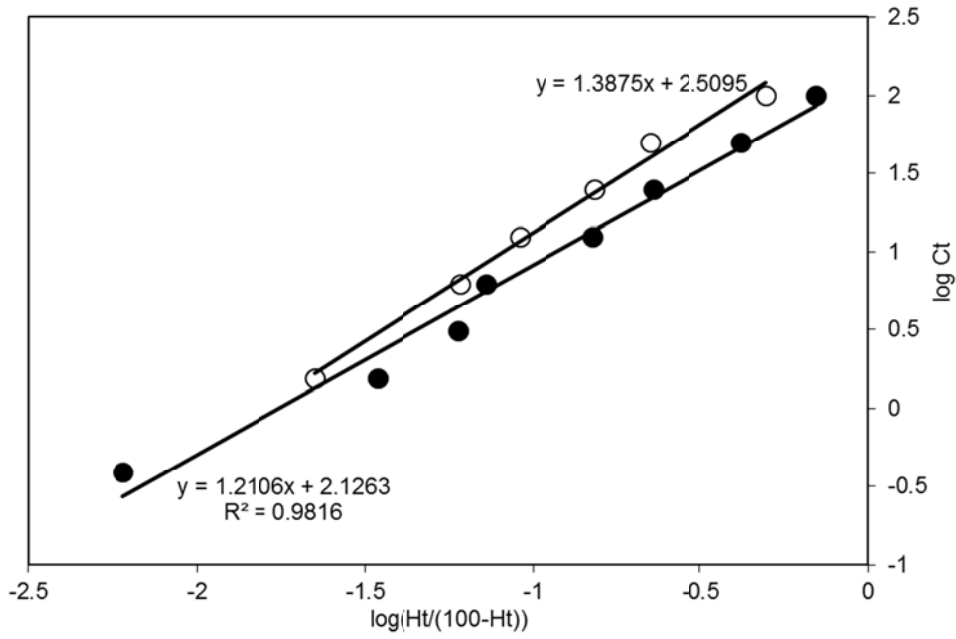


Figure S13. Dose-response curves $\log(Ct)$ versus $\log(Ht / (100 - Ht))$ for EC_{50} and EC_{20} value calculations of DPG toxicity using Microtox[®] test. See text S1 for calculation details. The two different symbols correspond to two replicate experiments.